

Bridge Deck Evaluation Using Portable Seismic Pavement Analyzer (PSPA)

PB2002-100227



FINAL REPORT
June 2000

Submitted by

Dr. Nenad Gucunski
Assistant Professor

Dr. Ali Maher
Professor and Chairman

Dept. of Civil & Environmental Engineering
Center for Advanced Infrastructure & Transportation (CAIT)
Rutgers, The State University
Piscataway, NJ 08854-8014



NJDOT Research Project Manager
Mr. Nicholas Vitillo

In cooperation with

New Jersey
Department of Transportation
Division of Research and Technology
and
U.S. Department of Transportation
Federal Highway Administration

Disclaimer Statement

"The contents of this report reflect the views of the author(s) who is (are) responsible for the facts and the accuracy of the data presented herein. The contents do not necessarily reflect the official views or policies of the New Jersey Department of Transportation or the Federal Highway Administration. This report does not constitute a standard, specification, or regulation."

The contents of this report reflect the views of the authors, who are responsible for the facts and the accuracy of the information presented herein. This document is disseminated under the sponsorship of the Department of Transportation, University Transportation Centers Program, in the interest of information exchange. The U.S. Government assumes no liability for the contents or use thereof.

1. Report No. FHWA 2000-05	2. Government Accession No.	3. Recipient's Catalog No.	
4. Title and Subtitle Bridge Deck Evaluation Using Portable Seismic Pavement Analyzer (PSPA)		5. Report Date March 2000	
		6. Performing Organization Code CAIT/Rutgers	
7. Author(s) Dr. Nenad Gucunski and Dr. Ali Maher		8. Performing Organization Report No. FHWA 2000-05	
9. Performing Organization Name and Address New Jersey Department of Transportation CN 600 Trenton, NJ 08625		10. Work Unit No.	
		11. Contract or Grant No.	
12. Sponsoring Agency Name and Address Federal Highway Administration U.S. Department of Transportation Washington, D.C.		13. Type of Report and Period Covered Final Report 9/11/1998 - 12/31/2000	
		14. Sponsoring Agency Code	
15. Supplementary Notes			
16. Abstract The primary objective of this study was to evaluate the capabilities of the Portable Seismic Pavement Analyzer (PSPA) device to evaluate the bridge deck elastic moduli and the deck thickness, and to detect and quantify concrete bridge deck delamination. The PSPA is a device for nondestructive evaluation of concrete bridge decks and pavements developed at the University of Texas at El Paso and produced by Geomeia Research and Development, Inc., El Paso, Texas. The PSPA device was designed and constructed as an extension result of the development of the Seismic Pavement Analyzer (SPA) for the sole purpose to provide information about the top layer of the pavement or a bridge deck. Primary applications of the device are in quality assurance/quality control of the top pavement layer, void detection, bridge deck delamination, and monitoring of concrete curing. To conduct these tasks, the PSPA relies on two ultrasonic methods in material characterization, and impact echo (IE) method in defect detection. The PSPA, with its ability for high level diagnosis of bridge decks, presents an essential tool to transportation and bridge engineers in administration and management of concrete deck bridges, i.e. in proper planning of their repair and rehabilitation.			
17. Key Words Portable Seismic Pavement Analyzer, PSPA, pavement, bridge deck delamination, nondestructive, asphalt		18. Distribution Statement	
19. Security Classif. (of this report) Unclassified	20. Security Classif. (of this page) Unclassified	21. No of Pages 70	22. Price

TABLE OF CONTENTS

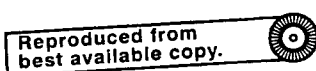
Chapter 1 - Introduction	1
Chapter 2 - Seismic Methods for Bridge Deck Evaluation	4
Chapter 3 - Portable Seismic Pavement Analyzer (PSPA)	13
PSPA Hardware	13
PSPA Software	14
Chapter 4 - Field Implementation of PSPA	23
Data Collection	23
Data Presentation	25
Testing on Rt. I-495 near Union City, New Jersey	25
Testing on Rt. I-287S near Edison, New Jersey	29
Chapter 5 - Numerical Simulation of Seismic Testing on Bridge Decks	43
Finite Element Model	43
Effect of Receiver Positioning, Impact Source Function and Delamination Geometry	48
Simulation of Delamination Progression	52
Chapter 6 - Data Visualization	56
Chapter 7 - Conclusions and Recommendations	60
References	62

LIST OF FIGURES

	Page
Figure 2.1 UBW and IE in evaluation of elastic modulus and thickness of the surface layer.	5
Figure 2.2 Examples of USW and IE test records.	6
Figure 2.3 Schematic of the SASW test.	7
Figure 2.4 Dispersion curve obtained from the USW test.	8
Figure 2.5 IE test on a delaminated deck.	9
Figure 2.6 Condition assessment grades with respect to the deck delamination.	10
Figure 2.7 Time records and response spectra for solid (good) and delaminated (serious) decks.	11
Figure 3.1 Portable Seismic Pavement Analyzer (PSPA).	13
Figure 3.2 The bottom view of the "lunch box."	14
Figure 3.3 PSPA general/data acquisition menu	15
Figure 3.4 Summary of the PSPA menus.	16
Figure 3.5 Definition of slab dimensions and the test point location.	17
Figure 3.6 View waveforms option in acquisition submenu.	18
Figure 3.7 Bank 1 waveforms.	18
Figure 3.8 Time records review in PSPA.	19
Figure 3.9 Unsmoothed and smoothed phase curves and the dispersion curve. $g=.7$, $h=.0005$, $i=50$.	20
Figure 3.10 Unsmoothed and smoothed phase curves and the dispersion curve. $g=.7$, $h=.0005$, $i=10$.	21
Figure 3.11 Response spectrum from impact echo test.	22
Figure 4.1 Typical grid used in PSPA testing of bridge decks.	23
Figure 4.2 Evaluation of bridge decks by PSPA.	24
Figure 4.3 Condition assessment for the two left lanes of 6 th span of Rt. I-495 bridge.	26
Figure 4.4 Shear modulus distribution for the two left lanes of the 6 th span of Rt. I-495S bridge.	27
Figure 4.5 Condition assessment for the two right lanes of 6 th span of Rt. I-495S bridge deck.	28
Figure 4.6 Shear modulus distribution for the right two lanes of the 6 th span of Rt. I-495S bridge.	29
Figure 4.7 A schematic of the test areas on the Rt. I-287S bridge deck.	31
Figure 4.8 Condition assessment of Rt. I-287S bridge deck. Continuous format.	32
Figure 4.9 Condition assessment of Rt. I-287S bridge deck. Discrete format.	33
Figure 4.10 Typical spectra for four condition assessment grades.	34
Figure 4.11 Frequency and corresponding thickness spectra for a deck in fair condition.	35

Figure 4.12	Frequency and spectral surfaces for line A14-I14 of Rt. I-287S bridge deck.	36
Figure 4.13	Test lines for presented frequency and thickness spectral surfaces.	37
Figure 4.14	Thickness spectral surface for sections A13-I-13, A16-I16 and A20-I-20.	39
Figure 4.15	Thickness spectral surfaces for sections D10-D20, G10-G20, and H10-H20.	40
Figure 4.16	Comparison of PSPA and chain drag condition assessment for a section of Rt. I-287S bridge deck.	41
Figure 5.1	Finite element models used in simulation of PSPA testing.	45
Figure 5.2	Typical acceleration histories for three receiver locations, $t=25$ cm, $d=15$ cm, $R=15$ cm.	46
Figure 5.3	Effect of clipping of surface waves on spectra. $T=25$ cm, $d=15$ cm, $R=15$ cm, $r=7.5$ cm.	47
Figure 5.4	Comparison of response spectra obtained from axisymmetric and plane strain models.	48
Figure 5.5	Comparison of clipped time records and time spectra for 25 and 75 mm receiver positions.	49
Figure 5.6	Comparison of time records and spectra for Model 1 with trapezoidal loading and Model 5 with haversine loading at radial distances of 25 and 75 mm.	50
Figure 5.7	Effect of the delamination position on spectra. $T=25$ cm, $R=15$ cm, $r=7.5$ cm.	51
Figure 5.8	Scenario 1. Changes in the response spectrum due to delamination expansion.	53
Figure 5.9	Scenario 2. Changes in the response spectrum due to progressive linking. $T=25$ cm, $d=15$ cm, $R=15$ cm, $r=7.5$ cm.	54
Figure 5.10	Scenario 2. Changes in the response spectrum due to Progressive linking. $T=25$ cm, $d=15$ cm.	55
Figure 6.1	3-Dimensional thickness spectrum for a bridge deck section.	56
Figure 6.2	3-Dimensional thickness spectrum for a section of the Rt. I-287S bridge deck.	58
Figure 6.3	3-Dimensional thickness spectrum for a section of the Rt. I-287S bridge deck.	59

**PROTECTED UNDER INTERNATIONAL COPYRIGHT
ALL RIGHTS RESERVED
NATIONAL TECHNICAL INFORMATION SERVICE
U.S. DEPARTMENT OF COMMERCE**



ACKNOWLEDGMENTS

This project was conducted in cooperation and under sponsorship of the New Jersey Department of Transportation (NJDOT). The principal investigators express their gratitude to the NJDOT for funding the research described herein. They are especially thankful to the project manager Mr. Nicholas Vitillo for his assistance in the organization of field testing, and valuable comments in the definition of the project objectives and the scope of the research. Contribution of Rutgers doctoral students Mrs. Vedrana Krstic, in the field investigation part, and Mr. Strahimir Antoljak, in the finite element modeling part, is gratefully acknowledged.

CHAPTER 1

INTRODUCTION

Post-construction monitoring of bridge decks is essential in detection of symptoms of deterioration at early stages, and thus for their economic management. To perform this task, methods used in evaluation should be both fast and accurate, and nondestructive. One of the most common problems in concrete bridge decks is a corrosion induced deck delamination. The current practice of deck inspection by chain dragging can provide information about the deck worsening condition only at stages when the delamination has already progressed to the extent that major rehabilitation measures are needed.

Three ultrasonic seismic techniques, namely ultrasonic body-wave (UBW), ultrasonic surface-wave (USW) and impact echo (IE), have been successfully implemented in evaluation of bridge decks (Sansalone, 1993; Gucunski and Maher, 1998), short and long term monitoring of pavement materials (Nazarian *et al.*, 1997; Rojas *et al.*, 1999) and other infrastructural systems (Sansalone and Street, 1997). The techniques were also successfully implemented in integrated devices for automated data collection and analysis (Nazarian *et al.*, 1997; Sansalone and Street, 1997). While the devices are fully capable of detecting deck delaminations at their various stages of progression, precise interpretation of the measured parameters is not fully automated and is somewhat dependent on the experience of the operator.

The device of special interest for this project is the Portable Seismic Pavement Analyzer (PSPA).

The PSPA is the state-of-the-art device for nondestructive evaluation of concrete bridge decks developed at the University of Texas at El Paso and produced by Geomedia Research and Development, Inc., El Paso. The PSPA device (Nazarian *et al.*, 1997) duplicates some of the capabilities of the Seismic Pavement Analyzer (SPA) (Nazarian *et al.*, 1993) in that it provides information only about the top layer of the pavement or a bridge deck. Primary applications of the device are in quality assurance/quality control of the top pavement layer, void detection, bridge deck delamination, and monitoring of concrete curing. The PSPA, with its ability for high level diagnosis of bridge decks, presents an essential tool to transportation and bridge engineers in administration and management of concrete deck bridges, i.e. in proper planning of their repair and rehabilitation. As illustrated in cited references, there are a number advantages of the PSPA in comparison to the traditional methods used in the inspection and quality control of bridge decks. The PSPA eliminates the need for extensive quality control of concrete based on strength tests on cylinders and drilled cores. Because the PSPA evaluates in-situ properties of the in-place concrete, it eliminates the need for correlation of differences in strengths of the in-place concrete and cylinders that may result from application of different placement, compaction and curing conditions. Similarly, while chain dragging can be used to determine locations that are critically deteriorated, the PSPA provides the ability for determining the onset of deterioration.

To improve its capabilities in bridge deck condition assessment, the New Jersey Department of Transportation (NJDOT) has requested from the Center for Advanced Infrastructure and Transportation (CAIT) evaluation and implementation of the PSPA device. This report summarizes the scope and results of that evaluation. The report is divided into six major sections. The first

section (Chapter 2) discusses the background and application of seismic methods in evaluation of bridge deck concrete. The second section (Chapter 3) discusses the PSPA device. The discussion concentrates on the hardware and software configurations, and provides instructions in the implementation of the device in the field and data reduction. The third section (Chapter 4) describes results of the PSPA field implementation, and represents the core of the report. Results from three bridge deck evaluations are presented. The fourth section (Chapter 5) includes results of a numerical simulation of bridge decks with delamination that was conducted for the purpose of evaluation of limitations of seismic methods in detection of delaminations and evaluation of their ability to detect changes in the deck condition for the purpose of long term monitoring. The fifth section (Chapter 6) includes a description and implementation of a developed three dimensional presentation of data collected by the PSPA device for a real time condition assessment of bridge decks. Finally, the sixth section (Chapter 7) includes conclusions of the investigations, recommendations for the implementation of the PSPA device in every day bridge deck evaluation operations, and recommendations for future research that will enhance the accuracy, simplicity and versatility of the device.

CHAPTER 2

SEISMIC METHODS FOR BRIDGE DECK EVALUATION

Seismic methods can be described as methods for evaluation of material properties and defects in structures that are based on generation of elastic waves and measurement of their velocity of propagation and other wave propagation phenomena, like reflections, refractions and dispersions. While there are many seismic techniques, of particular interest for bridge deck evaluation are three ultrasonic techniques: ultrasonic body-wave (UBW), ultrasonic surface-wave (USW) and impact echo (IE). UBW and USW techniques are used to measure velocity of propagation of compression (P) and surface (R) waves. The wave velocities are very well correlated to elastic moduli, and thus the two techniques can be described as a material quality control techniques. The IE technique is used to identify the depth of wave reflectors in a bridge deck or pavement structure, and thus is used to detect defects in the structure and can be considered to be a defect diagnostics tool.

Application of UBW and IE techniques in evaluation of a pavement or a bridge deck is described in Fig. 2.1, and illustrated by actual field test results in Fig. 2.2. In the first part of the evaluation the UBW test is conducted using an impact source and two receivers. From the travel time of the P-wave between two receivers, the P-wave velocity (V_p) is calculated. In the second part of the evaluation, the IE test is conducted using an impact source and a single nearby receiver. Because of a significant contrast in rigidity of concrete and a granular base of a pavement structure, or concrete and air in a case of a bridge deck, the elastic wave is nearly entirely being reflected between the bottom of the slab or discontinuity and the surface of the concrete layer or the deck. The frequency of reflections

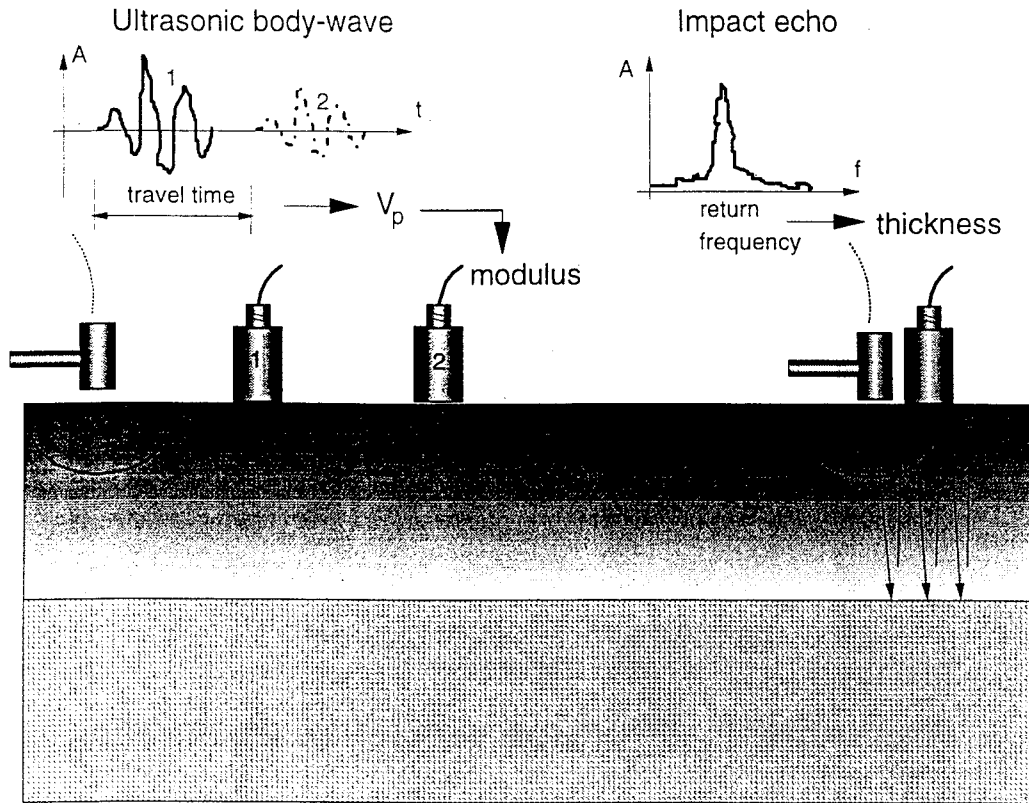


Figure 2.1. UBW and IE in evaluation of elastic modulus and thickness of the surface layer.

called return frequency is clearly visible in the response spectrum. The depth of the reflector, in this case the pavement layer or deck thickness, can be obtained from the return frequency and the previously determined P-wave velocity.

Because it is often difficult to identify arrivals of P-waves in an automated way, a more reliable way to estimate the P-wave velocity is through measurement of the R-wave velocity from the USW test. The USW test is identical to the spectral analysis of surface waves (SASW) test (Nazarian *et al.*, 1983; Stokoe *et al.*, 1994), except that the frequency range of interest is limited to a narrow high frequency range. The SASW test, depicted in Fig.2.3, utilizes a phenomenon of dispersion of surface

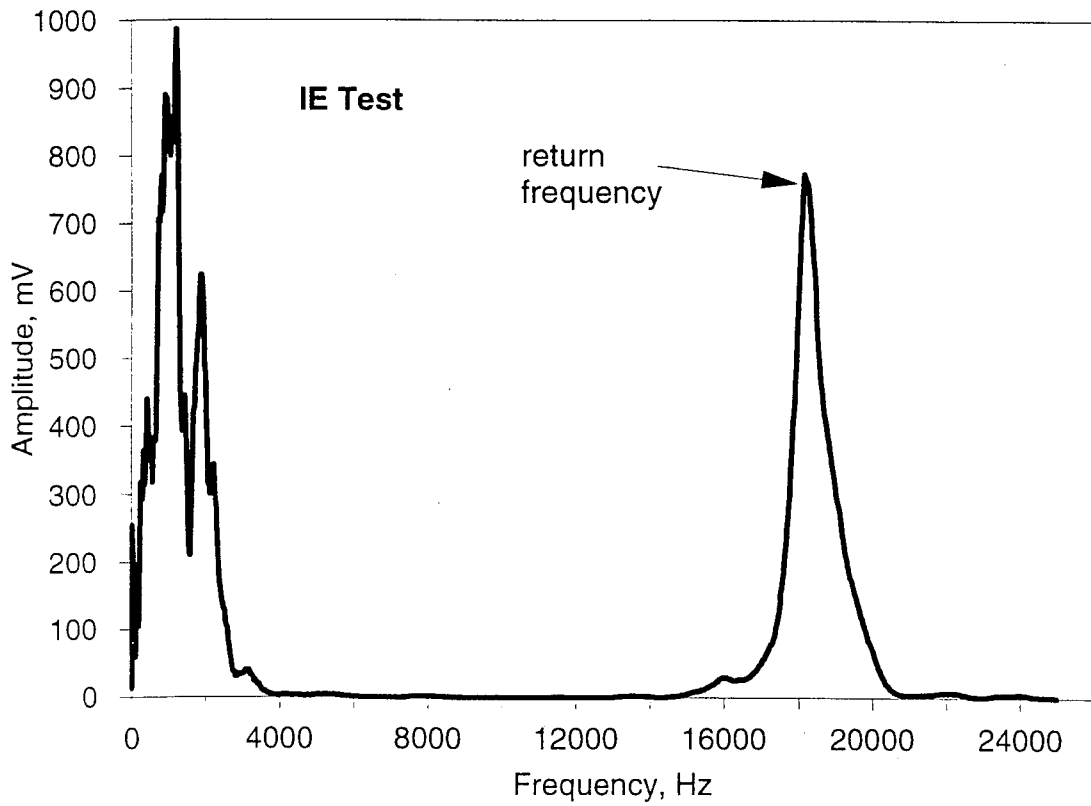
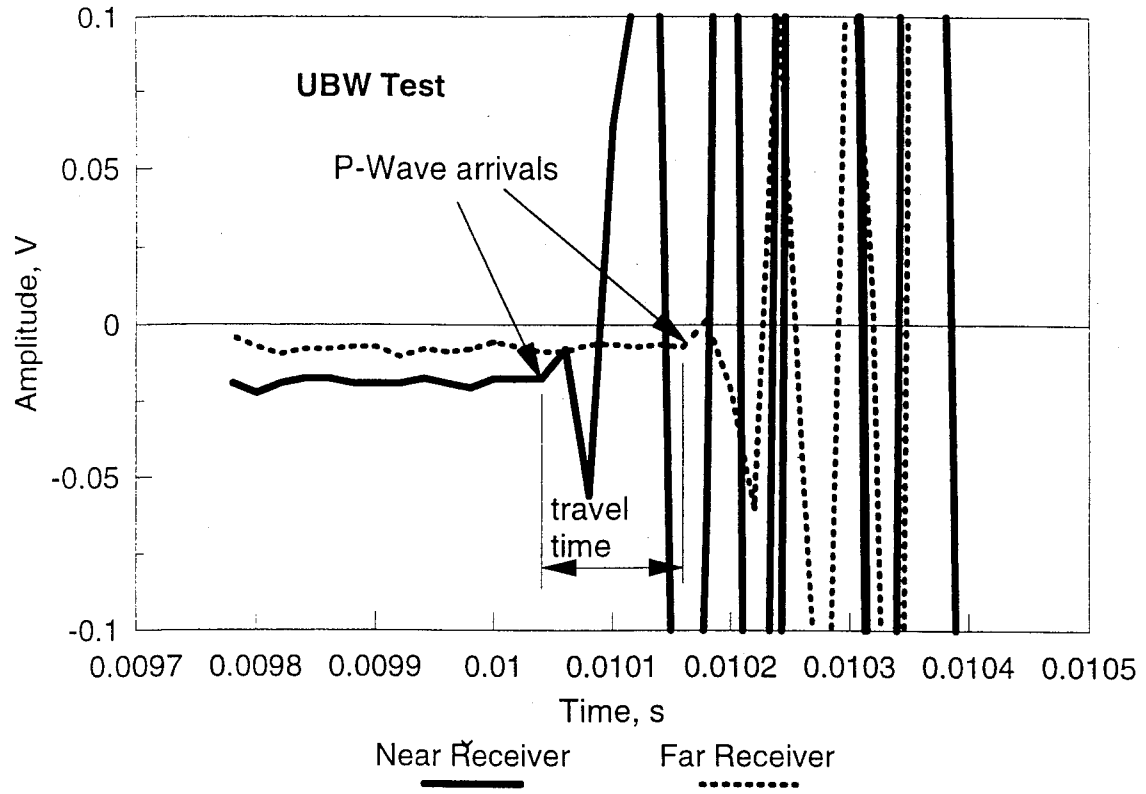


Figure 2.2. Examples of USW and IE test records.

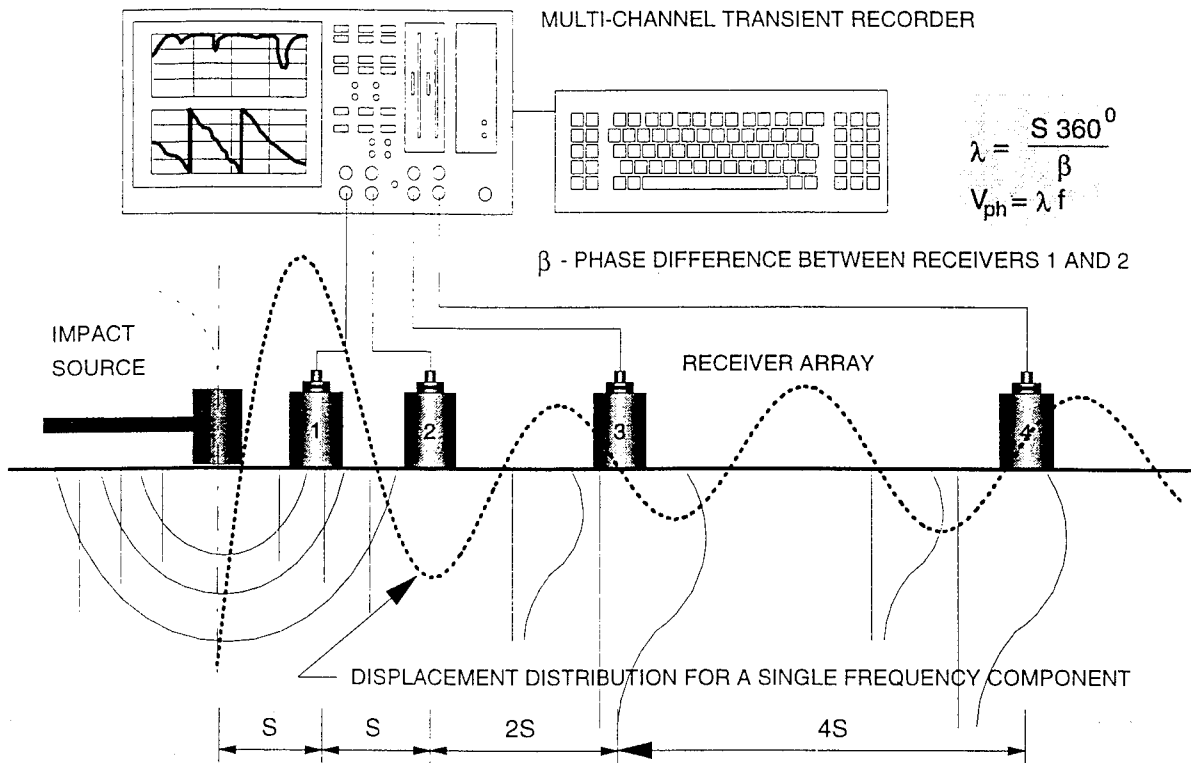


Figure 2.3 Schematic of the SASW test.

(R) waves in layered media, i.e. that waves of different frequencies propagate with different velocities. Surface waves are generated by an impact source, detected by a pair receivers, and recorded on an appropriate recording device. The objective of the test is to determine the surface wave velocity (phase velocity) - frequency relationship, described by the dispersion curve, and then from the dispersion curve, through the process of inversion or backcalculation, the elastic modulus profile of the system. The experimental dispersion curve for a single receiver spacing S is defined from the relationships presented in Fig. 2.3, where f represents frequency in Hz, and β the phase difference of a propagating wave between two receivers in degrees, obtained from the cross power spectrum of signals detected by the receivers. Using a crude approximation that the body of a R-wave extends to the depth of about one wavelength, it is obvious that the velocity of the R-wave

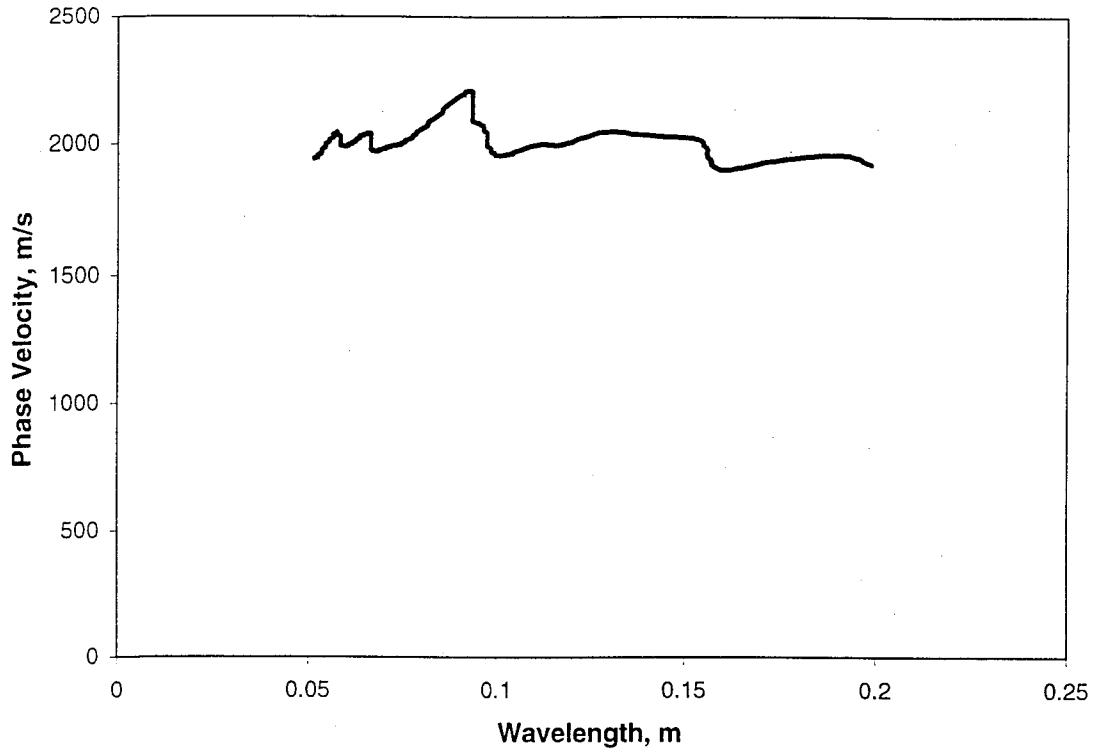


Figure 2.4. Dispersion curve obtained from the USW test.

(phase velocity) will vary, sometimes significantly, for wavelengths larger than the thickness of a surface layer due to propagation through materials of different properties. In the case of the USW method, only high frequency R-wave components are used in measurement. These components are of a wavelength shorter than the thickness of the surface layer, thus affected only by properties of the layer, and thus do not vary significantly with frequency. A typical dispersion curve obtained from the USW test is illustrated in Fig. 2.4. Once the R-wave velocity is determined it can be well correlated to both compression and shear (S) wave (V_s) velocities, and thus to the Young's and shear moduli. These correlations are given in Eqs. 2.1 to 2.4,

$$G = \rho V_s^2 \quad (2.1)$$

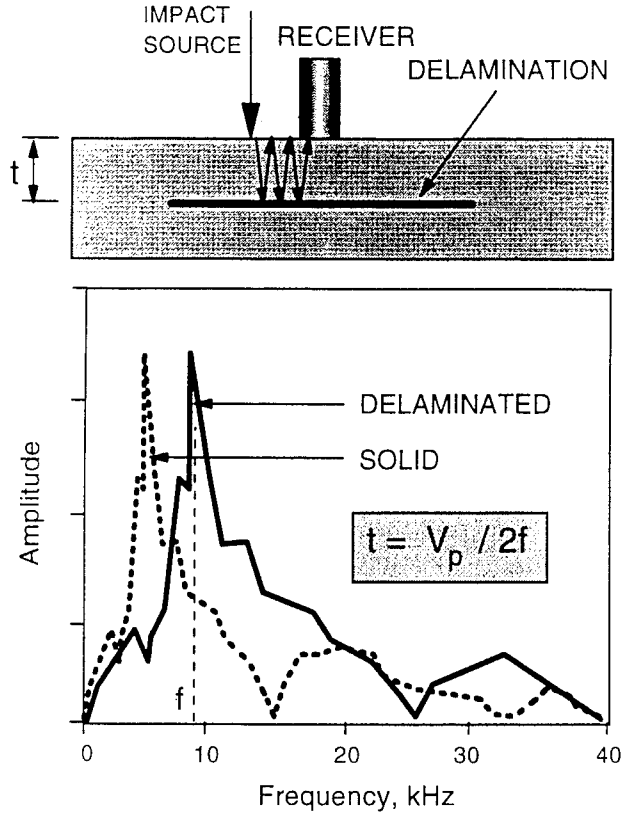


Figure 2.5. IE test on a delaminated deck.

$$E = 2\rho V_s^2(1 + \nu) \quad (2.2)$$

$$V_s = (1.13 - 0.16\nu)V_{ph} \quad (2.3)$$

$$V_p = V_s \sqrt{(2 - 2\nu) / (1 - 2\nu)} \quad (2.4)$$

where G is shear modulus, E Young's modulus, ρ mass density, ν Poisson's ratio and V_{ph} the phase velocity from the USW test corresponding to the R-wave velocity.

Primary objectives in bridge deck testing are evaluation of material properties and condition assessment with respect to a possible bridge deck delamination. As shown in Fig. 2.5, in a case of

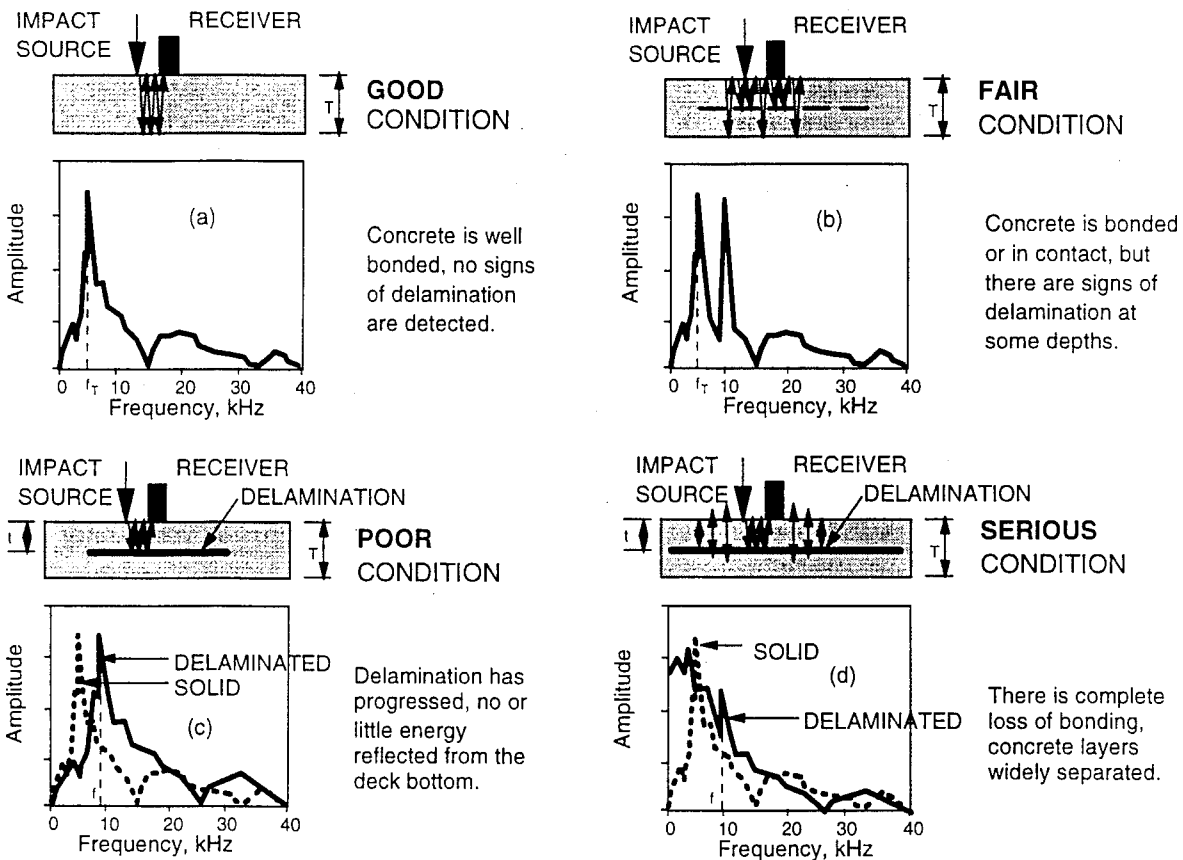


Figure 2.6. Condition assessment grades with respect to the deck delamination.

a delaminated deck, reflections of the P-wave occur at shallower depths, causing a shift of the peak in the response spectrum (return frequency) with respect to the peak for a sound deck towards higher frequencies due to a shorter travel distance. The depth of the reflector, the delamination in this case, is calculated according to the equation in the figure. Depending on the extent and continuity of the delamination, the partitioning of energy of elastic waves may vary and different grades as a part of the condition assessment can be assigned to that particular section of a deck. This is illustrated in Fig. 2.6. In the case of a sound deck (good condition - Fig. 2.6a) a distinctive peak in the response spectrum, corresponding to the full depth of the deck, can be observed. Initial delamination (fair condition - Fig. 2.6b) is described as occasional separations or horizontal cracking between the two

deck zones. It can be identified through a presence of two distinct peaks: the first one corresponding to reflections from the bottom of the deck, the second corresponding to reflections from the delamination. The presence of two peaks is an indication of radiation of a portion of elastic wave energy towards the bottom of the deck. Progressed delamination (poor condition - Fig. 2.6c) is characterized by a single peak at a frequency corresponding to reflections from a reflector shallower than the deck thickness, indicating that little or no energy is being propagated towards the bottom of the deck. Finally, in a very severe case of wide delamination (serious condition - Fig. 2.6d), the dominant response of the deck to an impact is characterized by a low frequency response (in an audible range) or by the flexural mode oscillations. It is significantly below the return frequency for

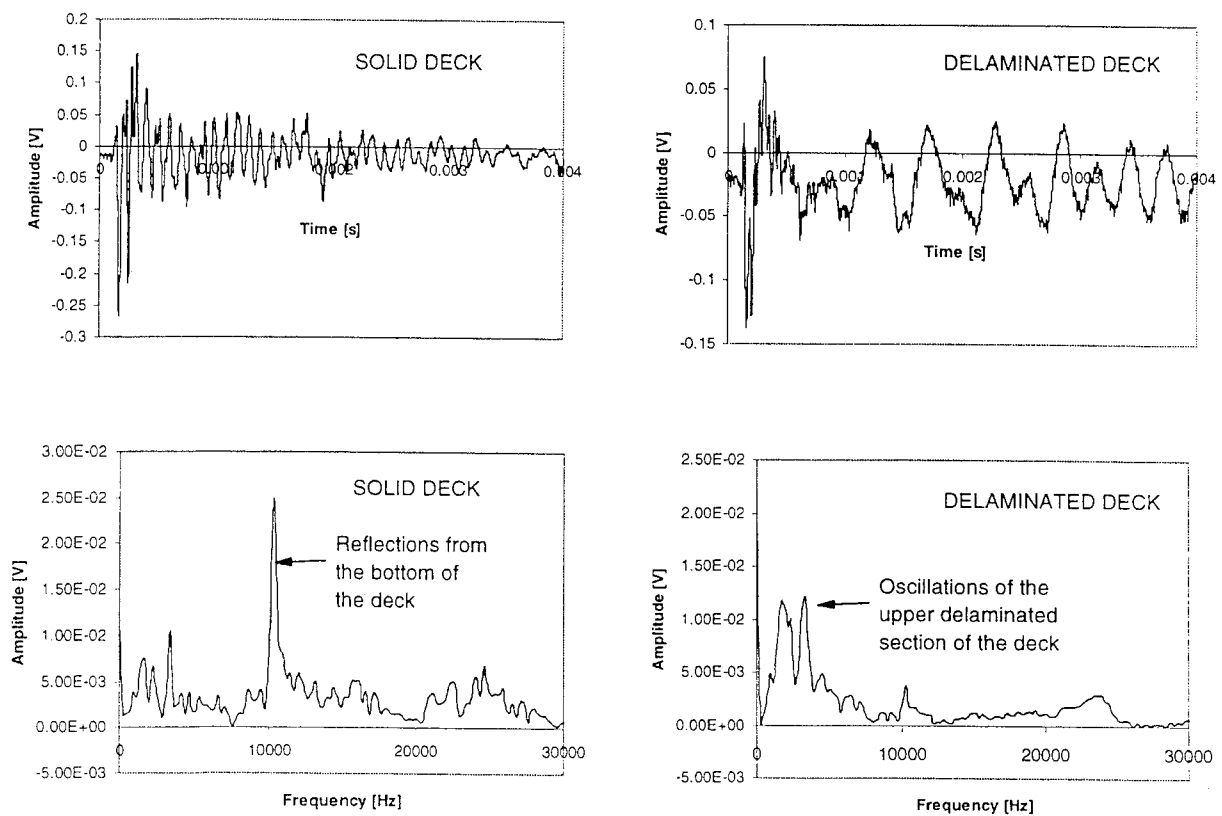


Figure 2.7. Time records and response spectra for solid (good) and delaminated (serious) decks.

the deck bottom, giving an apparent depth of the reflector larger than the deck thickness. Examples of records for good and serious conditions are presented in Fig. 2.7. The return frequency in the left hand side spectrum is 10.5 kHz. From a previously determined V_p of 4050 m/s and the return frequency, a thickness of 19.2 cm is measured matching very closely the design thickness of 20.3 cm. On the other hand, the dominant response in the right hand side spectrum can be observed in a range from approximately 1 to 4 kHz, defining apparently a large deck thickness and a serious condition.

CHAPTER 3

PORTABLE SEISMIC PAVEMENT ANALYZER (PSPA)

PSPA Hardware

The Portable Seismic Pavement Analyzer (PSPA) is manufactured by Geomeedia Research and Development (GR&D), Inc., El Paso, Texas. The PSPA was developed as an extension of the Seismic Pavement Analyzer development (Nazarian *et al.*, 1993), as a device with a sole purpose of evaluation of the surface pavement layer and bridge decks. The device integrates the three ultrasonic techniques (UBW, USW, IE). As illustrated in Figs. 3.1 and 3.2, the device consists of three main elements. The core of the system is a "lunch box", a box containing a solenoid type impact hammer and two high frequency accelerometers 7.5 and 21.5 cm away from the hammer in a tripod arrangement for better coupling of the hammer and accelerometers during testing. The

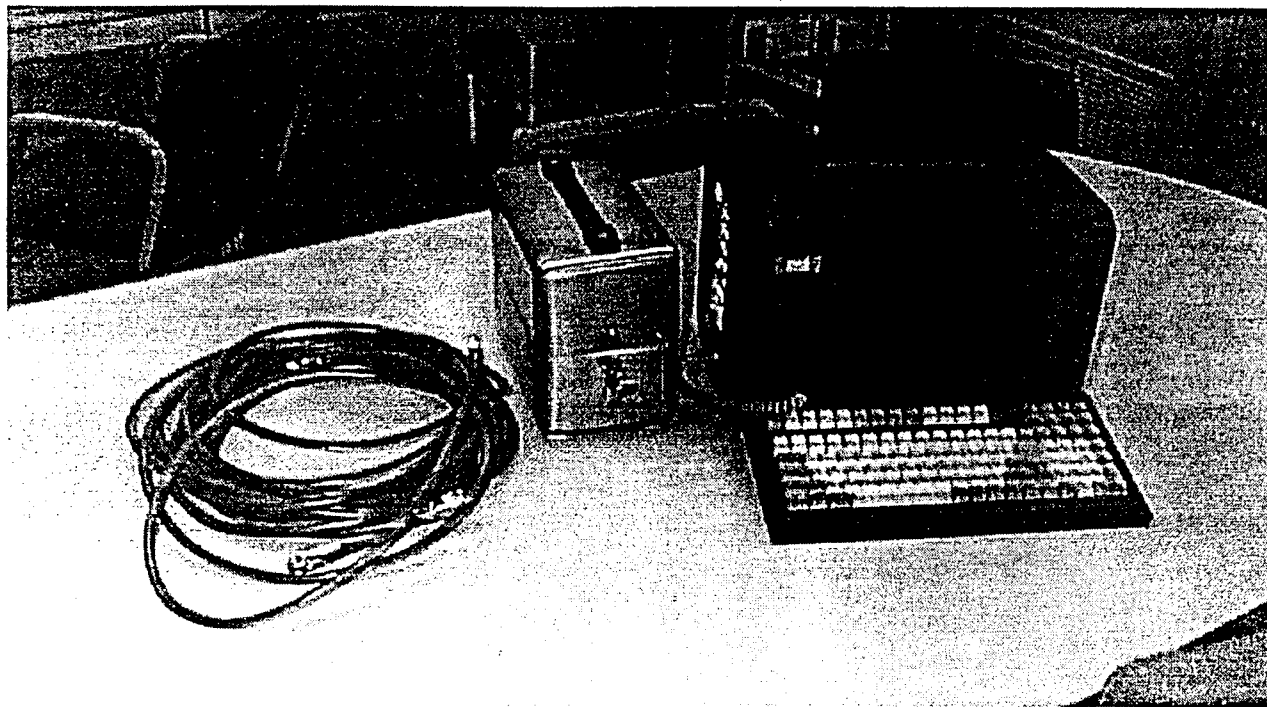


Figure 3.1. Portable Seismic Pavement Analyzer (PSPA).

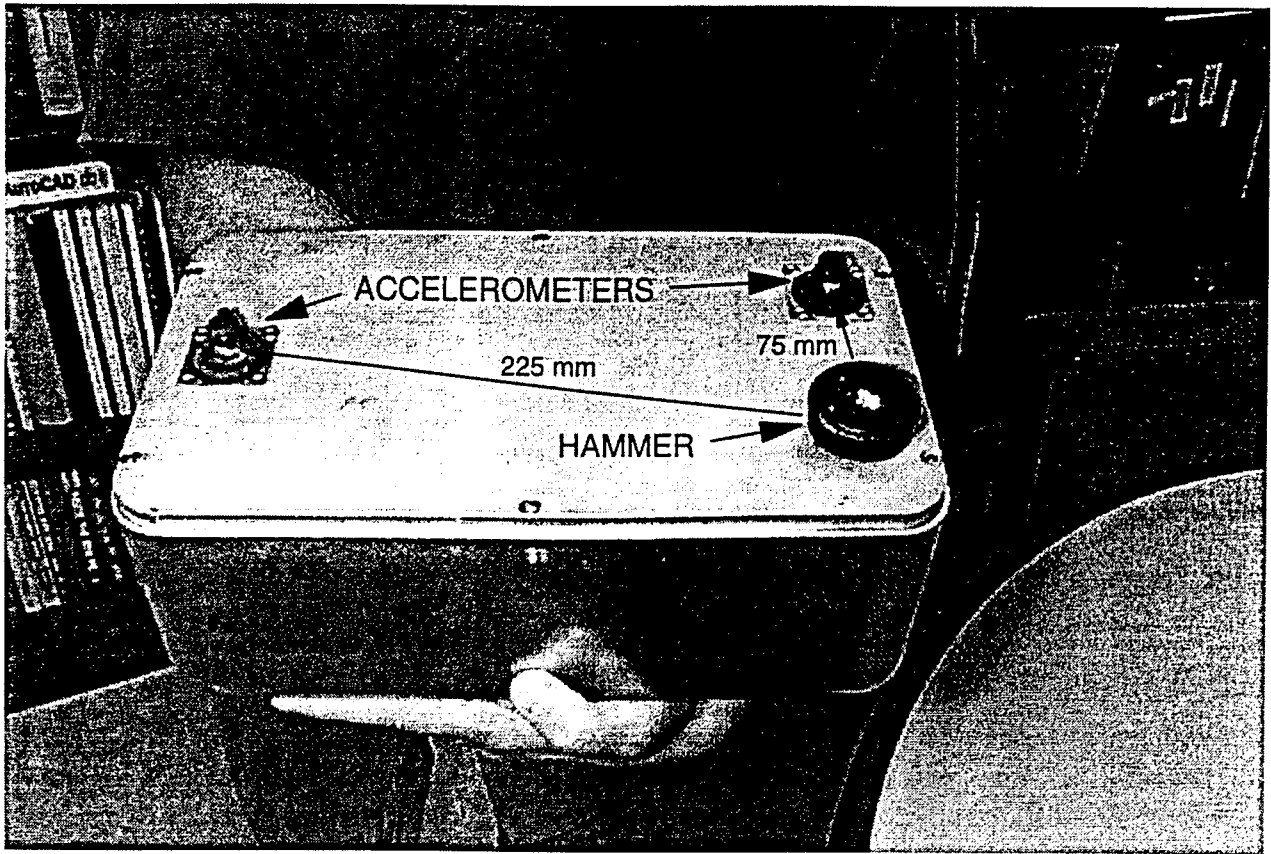


Figure 3.2 The bottom view of the “lunch box.”

impact source is a needle shaped hammer of an approximate diameter 1-2 mm. It can be calibrated to produce impacts of various duration, but the defaults setting calls for an impact of duration of approximately 50 μ s duration. The “lunch box” can be used on both horizontal and vertical surfaces. All controls and data acquisition are in a computer that is connected by a serial type cable to the “lunch box.”

PSPA Software

One of the strong sides of the PSPA device is the flexibility of the design of the device that

allows use of both proprietary and non-proprietary (user developed) software in data reduction, analysis and interpretation. Two sets of programs were used in the evaluation of the PSPA device. The first program used is program PSPA. The primary usage of the program includes PSPA controls field data acquisition, and preliminary material quality and condition assessment. The second program is program PSPAA. It is used for more precise data postprocessing. Finally, it should be mentioned that, since accelerometer time histories can be easily extracted from the PSPA, a number of commercial programs for signal processing, like DaDisp, Matlab or Maple can be used in data analysis and interpretation. Since there are no manuals, except for help files provided by Geomeia Research and Development, Inc., the following paragraphs discuss in more details implementation of PSPA and PSPAA programs in data acquisition, analysis and interpretation.



Figure 3.3. PSPA general/data acquisition menu.

The basic look of the PSPA program menu is presented in Fig. 3.3. There are five basic operations of the program: data acquisition, data review and reanalysis, device and project setup, device calibration and help. Each of these five main options has a set of submenus that are summarized in Fig. 3.4. The description follows a typical sequence of tasks in field implementation of the device and data reanalysis. The first step in the field implementation is the selection or definition of the project setup. It includes the description of the project, selection of the message level and type of operation (remote or local), and a definition of the expected surface pavement layer or bridge deck structure in terms of the ranges of elastic moduli and layer thickness. The setup also allows for the definition of the default size of a pavement slab and position of the PSPA test point on the slab. This

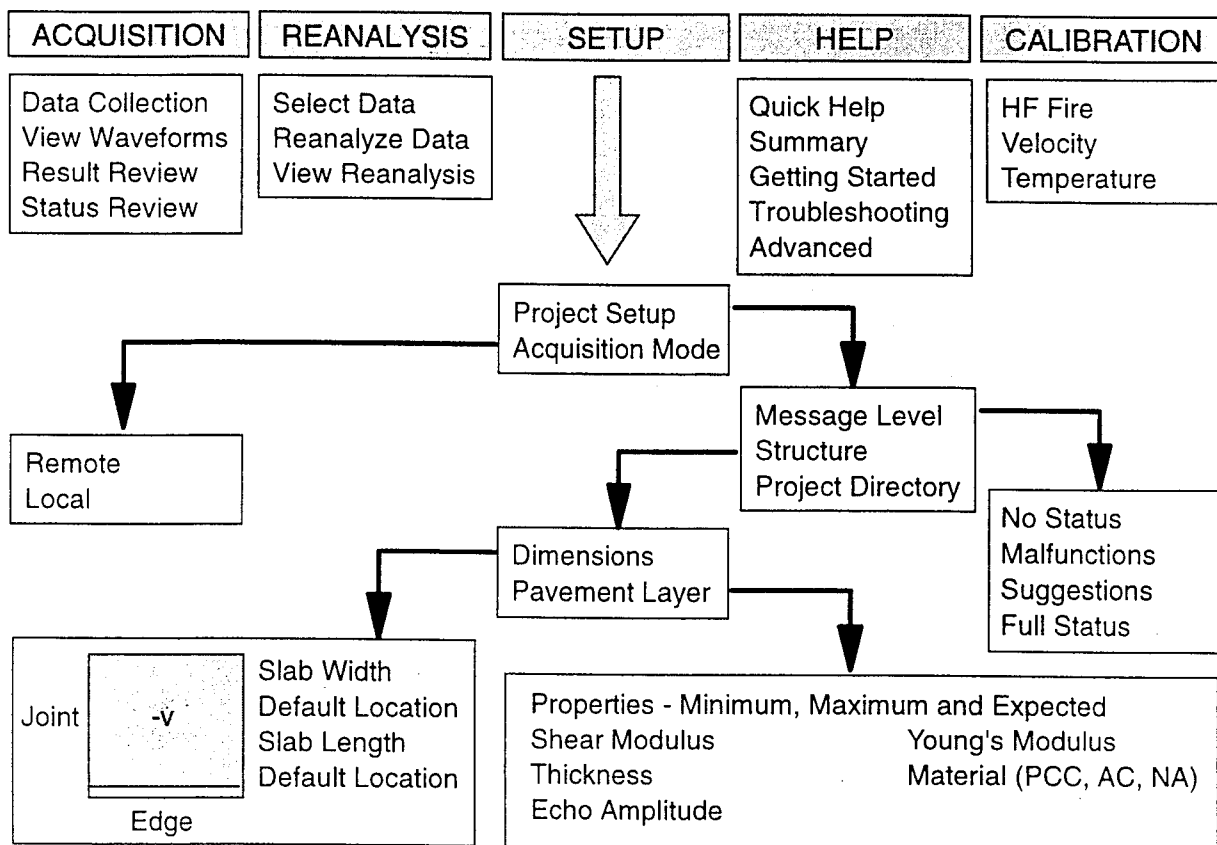


Figure 3.4. Summary of the PSPA menus.

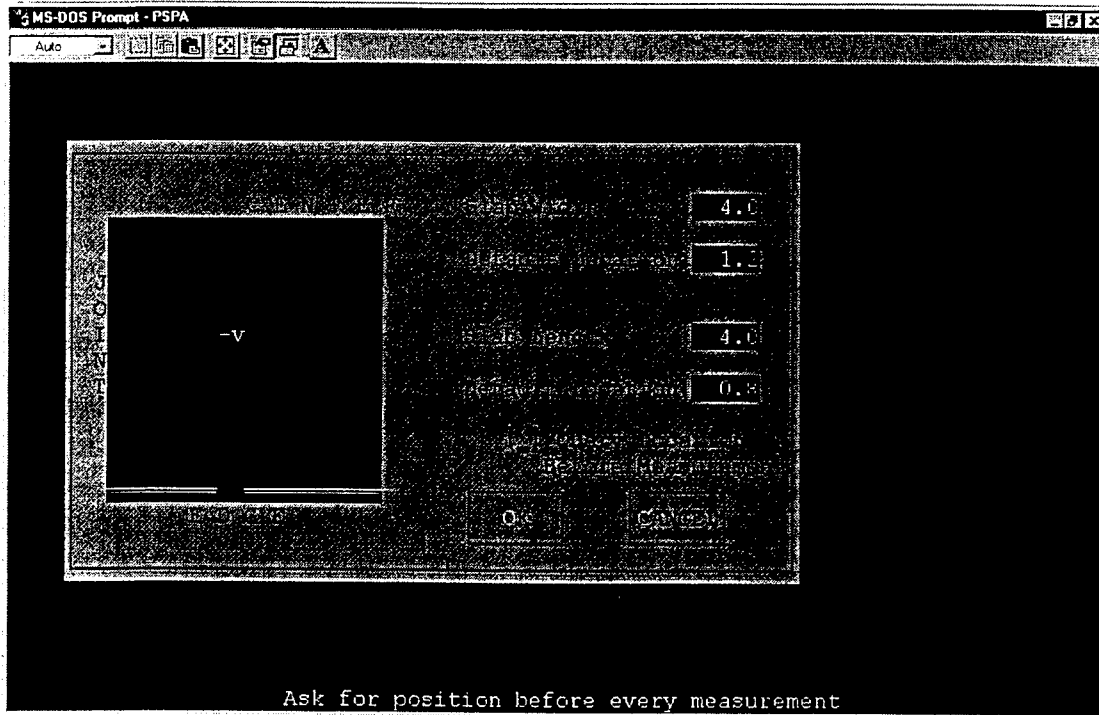


Figure 3.5. Definition of slab dimensions and the test point location.

is illustrated in Fig. 3.4 at the left bottom corner and in Fig. 3.5, where symbols -v are used to identify the location of the PSPA and the orientation of the receiver array.

Once the project and the expected structure is defined, the data are collected by simple selecting the data collection option in the acquisition submenu. The duration of the data collection takes about 15 seconds, during which period the system has collected two sets of records, each set consisting of data for three hammer impacts. Collected data can be reviewed using the view waveforms option. This is illustrated in Fig. 3.6 where bank0 and bank1 represent the two sets of records. Each set of the records can be examined for two purposes, as it is illustrated for bank1 in Fig. 3.7. The first purpose is to examine the whether the shape of the signal corresponds to typically obtained signals. The second purpose it examine the repeatability of the signal. As presented in Fig. 3.7 signals from three

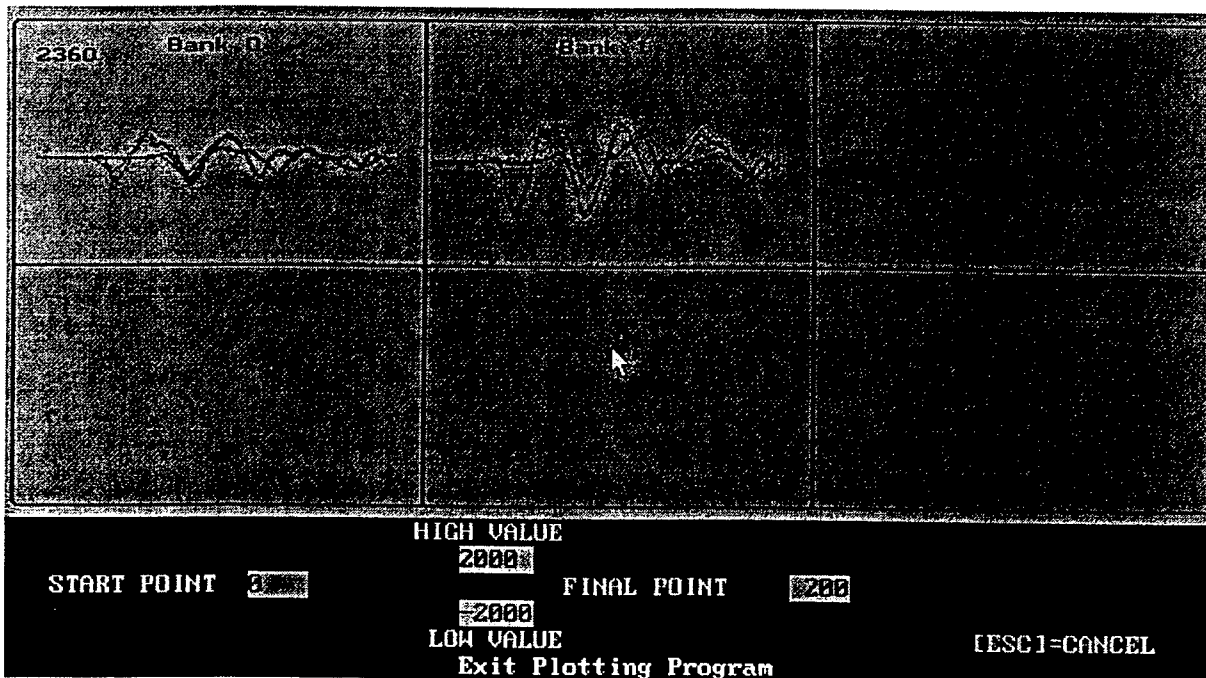


Figure 3.6. View waveforms option in acquisition submenu.

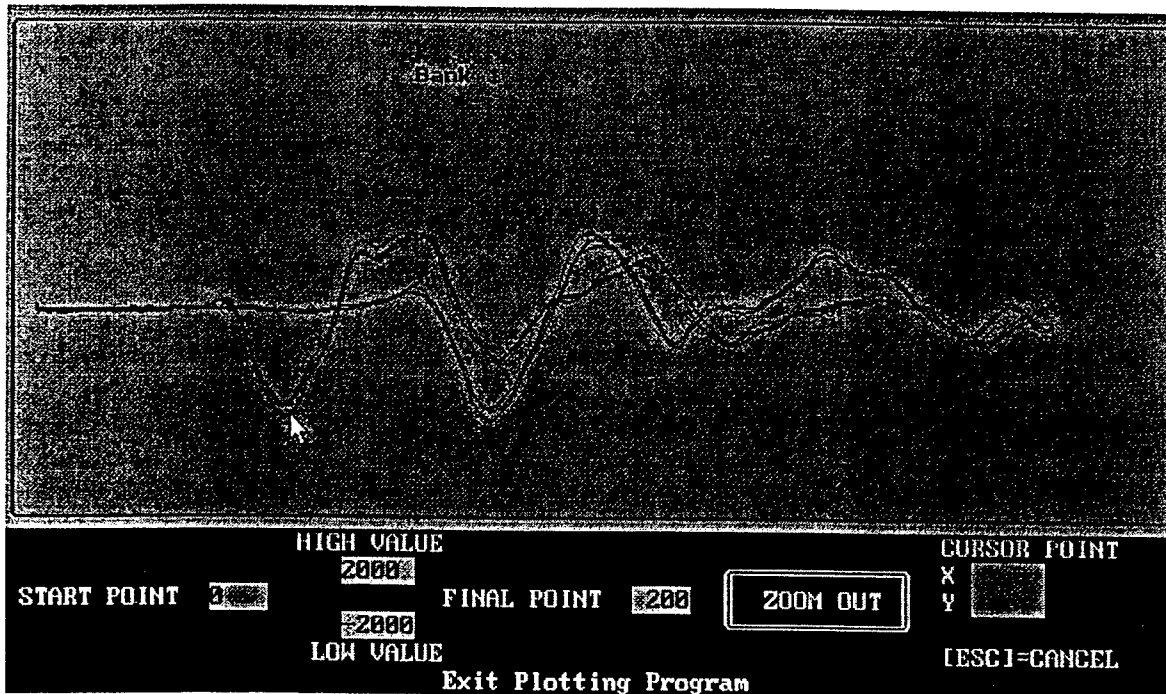


Figure 3.7. Bank 1 waveforms.

impacts overlap very well indicating high repeatability of the test. A number of options in the menu were primarily developed for the use with the Seismic Pavement Analyzer (SPA) and either are not implemented (like result review, status review), not implemented in the standard version of the PSPA program (like calibrations) or are better done using the PSPAA program (like reanalysis).

PSPAA postprocessing/reanalysis program is used primarily to enhance the development of the dispersion curve for the purpose of evaluation of the shear wave velocity (shear modulus), and to analyze the impact echo spectrum for the purpose of the delamination degree based condition assessment. PSPAA consists of several routines for examination of time records and response spectra

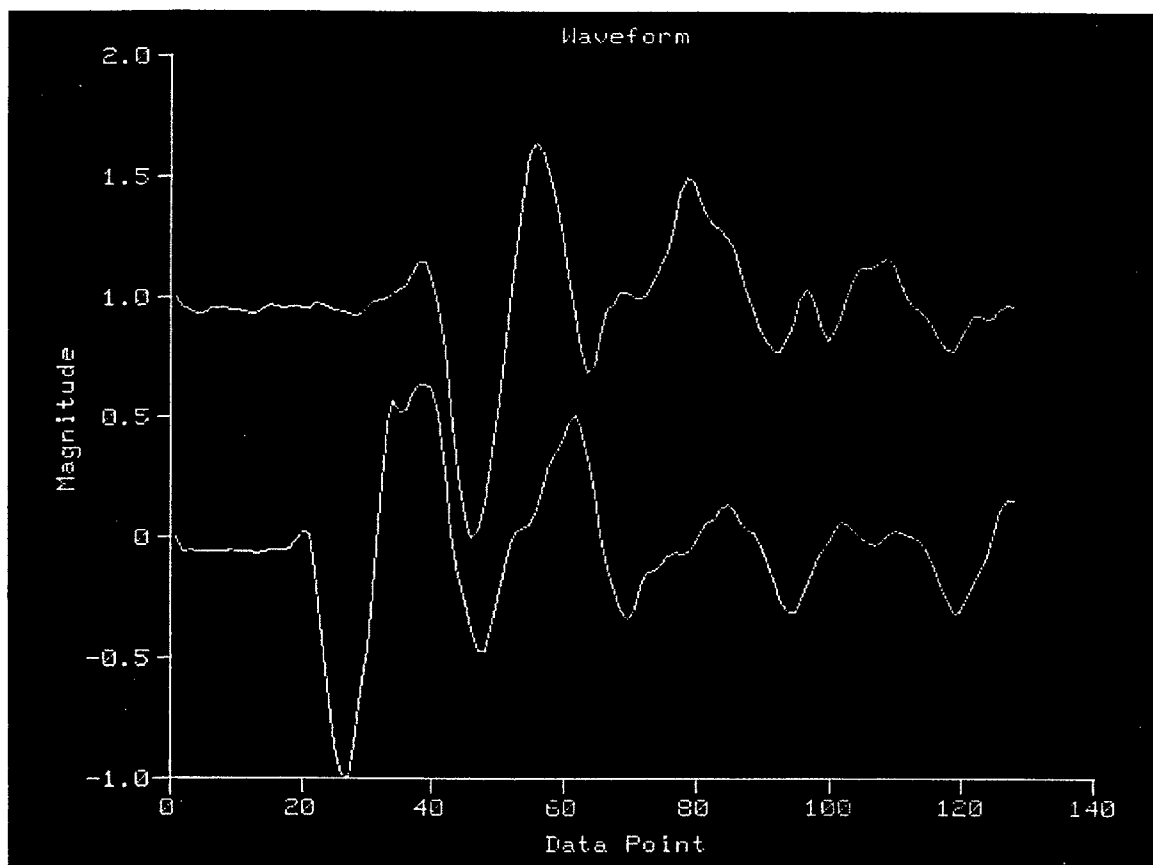


Figure 3.8. Time records review in PSPAA.

and derivation of the dispersion curves. The routine can be easily added or removed from the program depending on objectives of the reanalysis. The following is the typical flow of the reanalysis. It starts with the extraction of time records from a previously compressed record and presentation of the predefined time record, for example of the third hit from bank1 as illustrated in Fig. 3.8. Again, as in PSPA program view waveform option, the primary objective of viewing time records is to estimate the quality of the recorded signal. PSPAA also allows for implementation of the view waveform routine presented in Figs. 3.6 and 3.7 for examination of the repeatability of the signal.

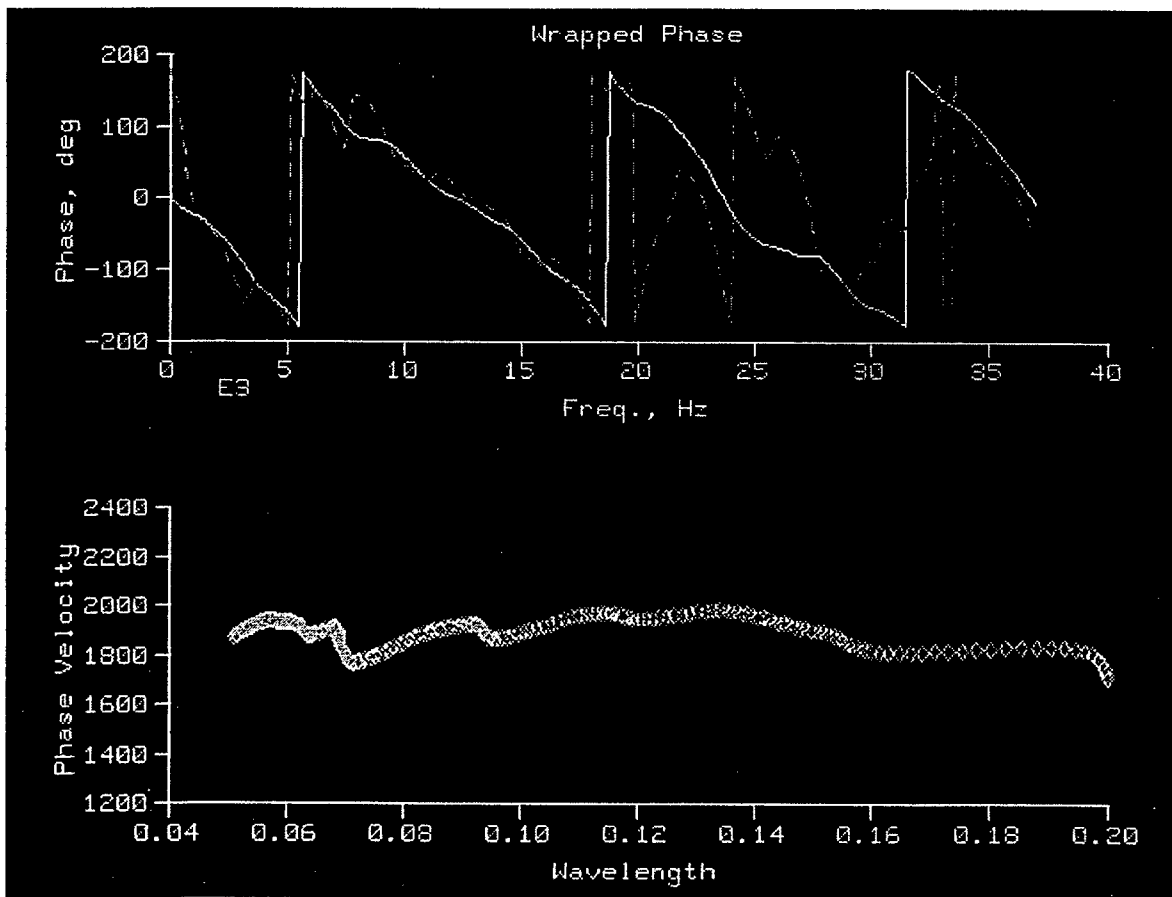


Figure 3.9. Unsmoothed and smoothed phase curves and the dispersion curve. $g=0.7$, $h=0.0005$, $i=50$

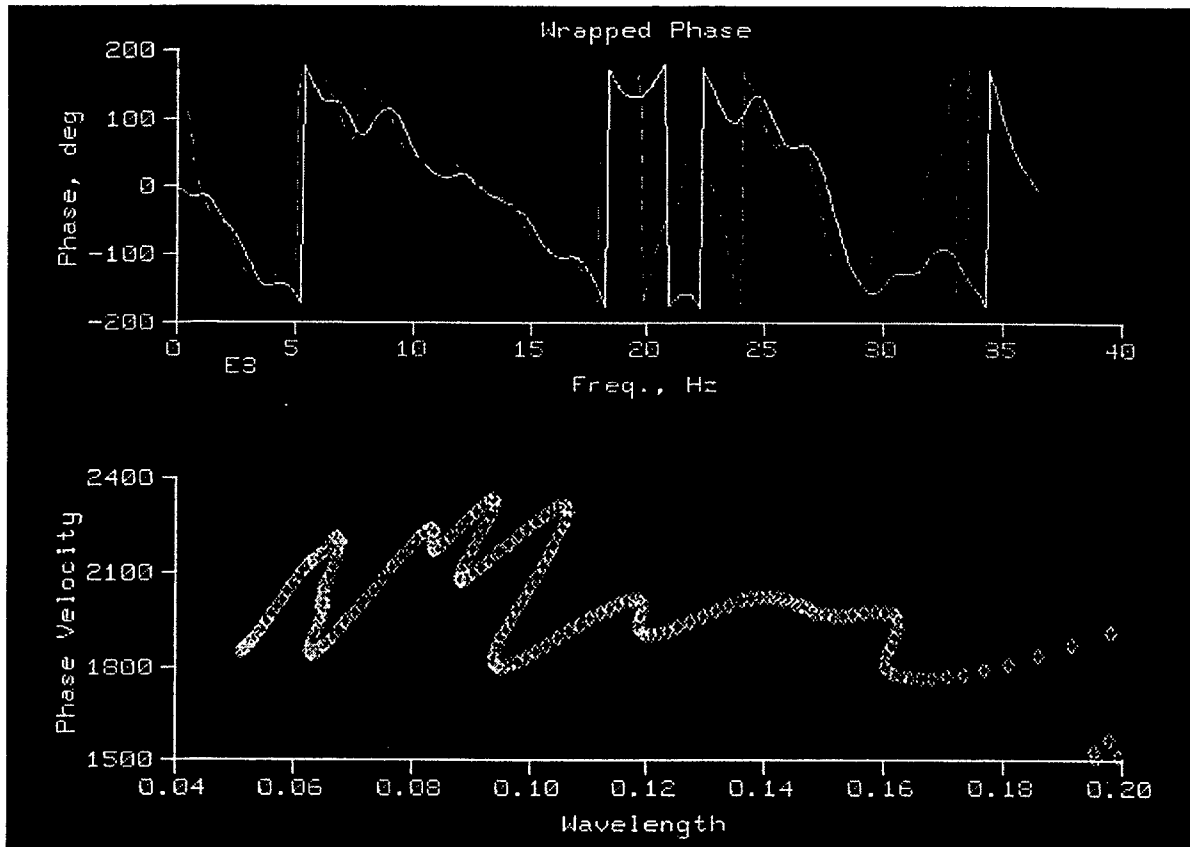


Figure 3.10. Unsmoothed and smoothed phase curves and the dispersion curve. $g=0.7$, $h=0.0005$ and $i=10$.

The second and maybe the most important routine assists in the development of the dispersion curve. As presented in Fig. 3.9, the routine plots the “unwrapped” phase of the cross power spectrum of signals at near and far receivers, compares it to a smoothed phase curve, and develops the dispersion curve from the smoothed phase. The unsmoothed phase curve is presented by a dashed line, while the smoothed curve by the full line. Smoothing of the phase can be controlled using three parameters: g , h and i . Parameters g , h and i control the weighing factor relative to the coherence, the slope of the phase curve and the closeness of the smoothed and experimental phase curves, respectively. Effect of parameter i is illustrated in Fig. 3.10, where g and h parameters were identical to those from Fig. 3.9. To develop the dispersion curve, the unwrapped phase curve first needs to be

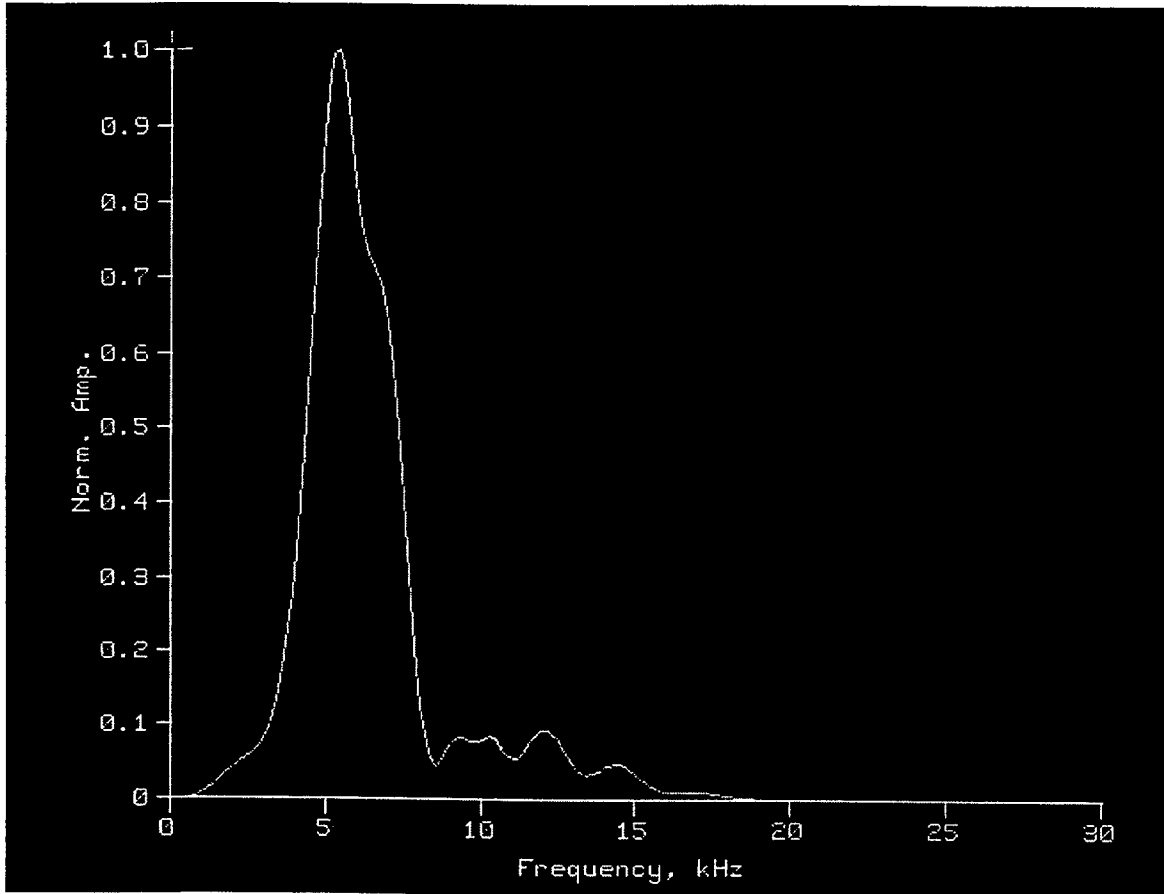


Figure 3.11. Response spectrum from impact echo test.

converted to a continuous format through the process of unwrapping or unfolding. Details about the unfolding can be found in Nazarian (1983), Gucunski (1991), Stokoe *et al.* (1994) and in a number of other references. Once the phase is in a continuous format, the dispersion curve can be obtained according to the relations described in Chapter 2, and the average phase velocity is calculated. The average phase velocity is used in the calculation of the shear wave velocity and elastic moduli according to Eqs. (2.1) to (2.3). Typically, the last routine of PSPAA program is presentation of the spectrum from the impact echo test. Return frequencies can be read and the condition assessment made according to the descriptions presented in Chapter 2 and summarized in Fig. 2.6. A typical spectrum from the impact echo test on a bridge deck is presented in Fig. 3.11.

CHAPTER 4

FIELD IMPLEMENTATION OF PSPA

Data Collection

Field evaluation of bridge decks is typically done on grids 0.6x0.6 m to 0.9x0.9 m, as illustrated in Fig. 4.1. The test at a single point is simple and takes less than 30 seconds. The “lunch box” is placed at the test point (Fig. 4.2), a series of impacts (6-10) of a 50 μ s duration is applied and accelerations recorded by a pair of accelerometers. The PSPA testing is fairly insensitive to traffic induced vibrations because of a high frequency range of interest, typically between 2 and 30 kHz.

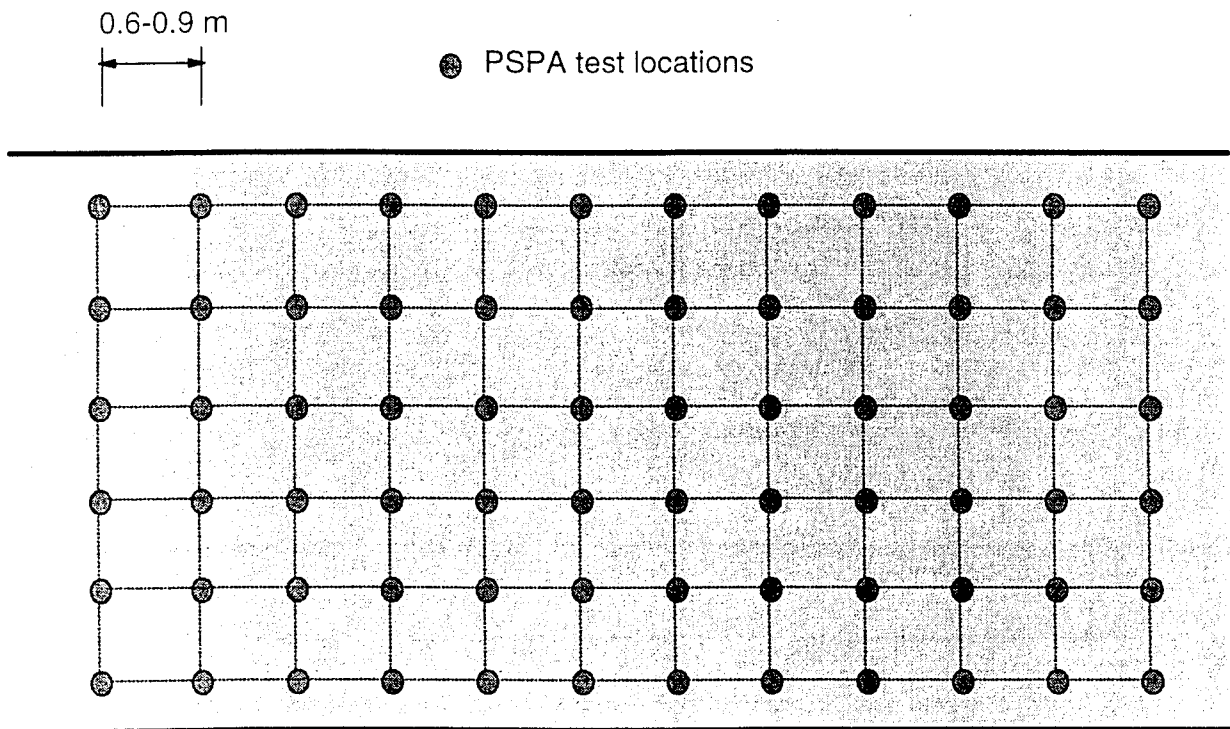


Figure 4.1. Typical grid used in PSPA testing of bridge decks.



Figure 4.2. Evaluation of bridge decks by PSPA.

Therefore, it does not require traffic interruptions, except a lane closure and traffic control for safety reasons. Experience from testing on several bridges and pavements is that in most cases testing at

a number of points needs to be repeated. The primary causes of the need for repeated testing are poor contact/coupling between accelerometers and the pavement/bridge deck surface and a poor impact application. The second one is caused by the hammer needle hitting either a void or a small aggregate grain in the pavement or bridge deck. The number of points retested depends on the roughness of the pavement/bridge deck surface. In most cases it can be estimated as 20 to 30% of the number of test points. In some extreme cases, as e.g. in a case of a highly grooved ultrathin white topping (UTW) the test at a single point needs to be repeated several times to obtain any useful data. GR&D is working on the resolution of the problem that involves modification of the size and the shape of the foot of the impact hammer.

Data Presentation

Results from PSPA testing are commonly described in terms of shear and Young's moduli (or P and S wave velocity) distributions, and condition assessment distributions (with respect to the degree of delamination). These distributions, as illustrated in the following sections on testing of two bridge decks, can be in a form of plan view and deck cross section distributions, or, as illustrated in Chapter 6, in terms of three dimensional translucent views into the bridge deck interior.

Testing on Rt. I-495 near Union City, New Jersey

The first example of evaluation of a bridge deck is for an overpass on Rt. I-495S near Union City, New Jersey. The evaluation was on done of both right and left lanes of the 6th span using a 0.75x0.75

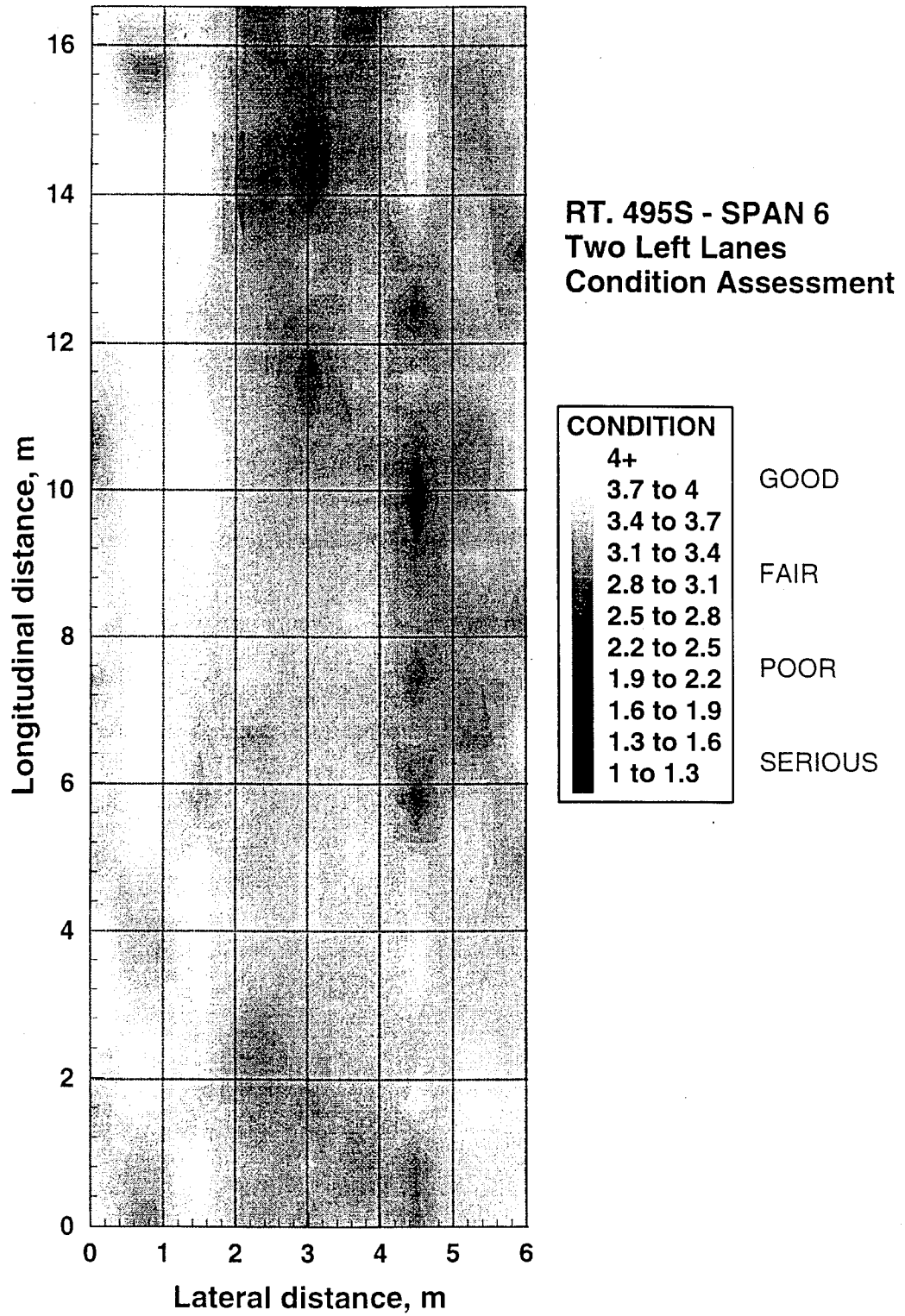


Figure 4.3. Condition assessment for the two left lanes of 6th span of Rt. I-495 bridge.

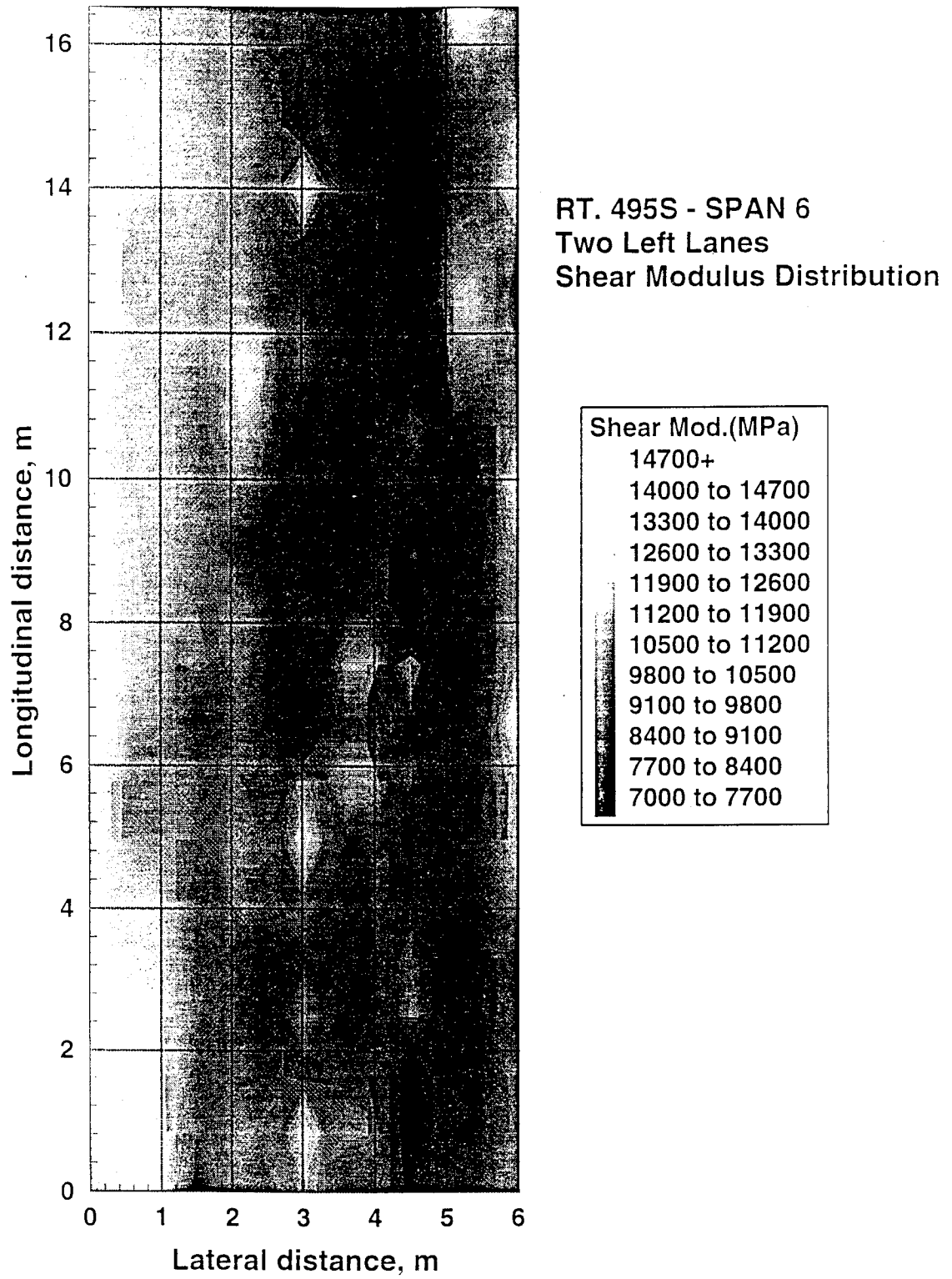


Figure 4.4. Shear modulus distribution for the two left lanes of the 6th span of Rt. I-495S bridge.

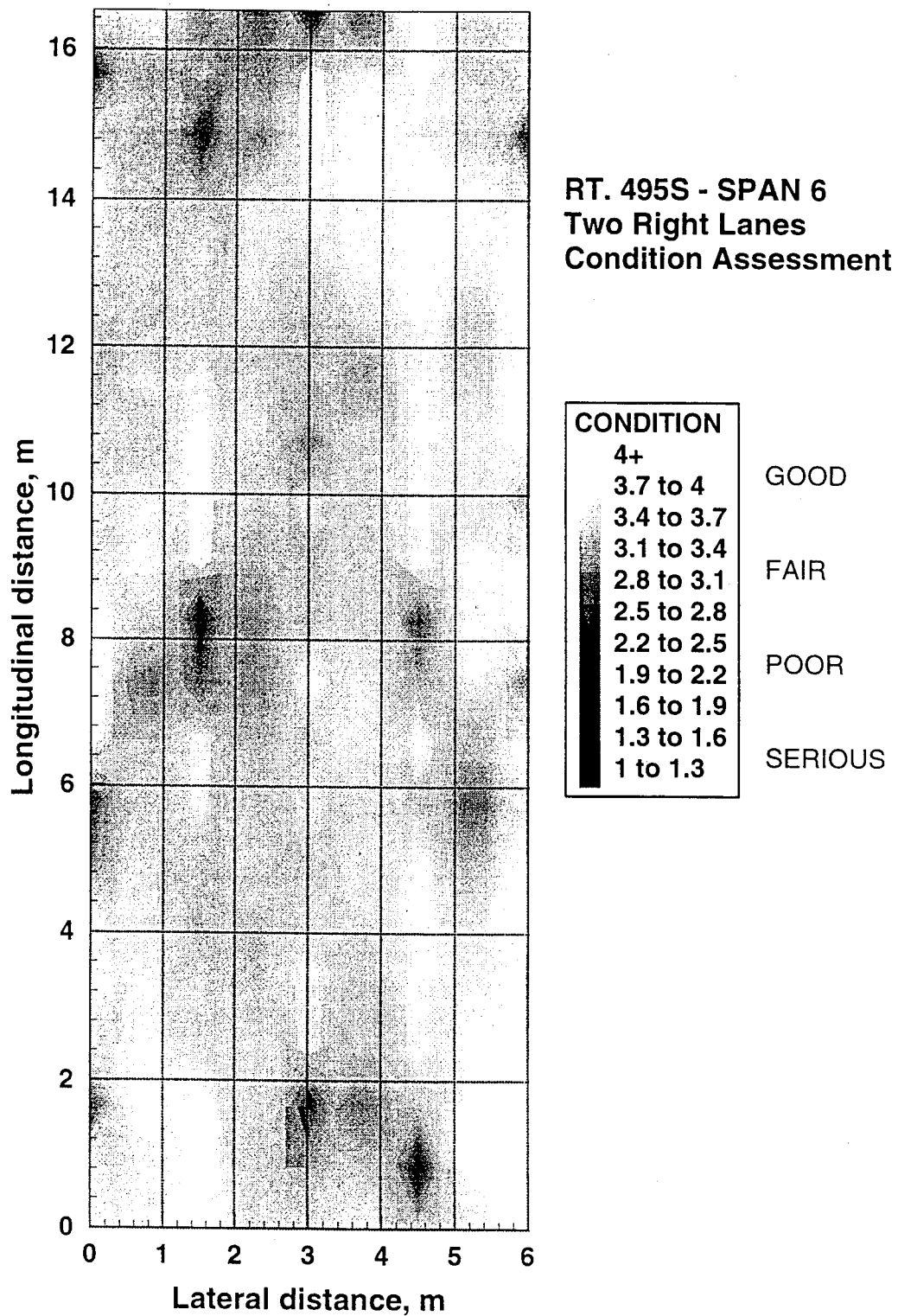


Figure 4.5. Condition assessment for the two right lanes of 6th span of Rt. I-495S bridge deck.

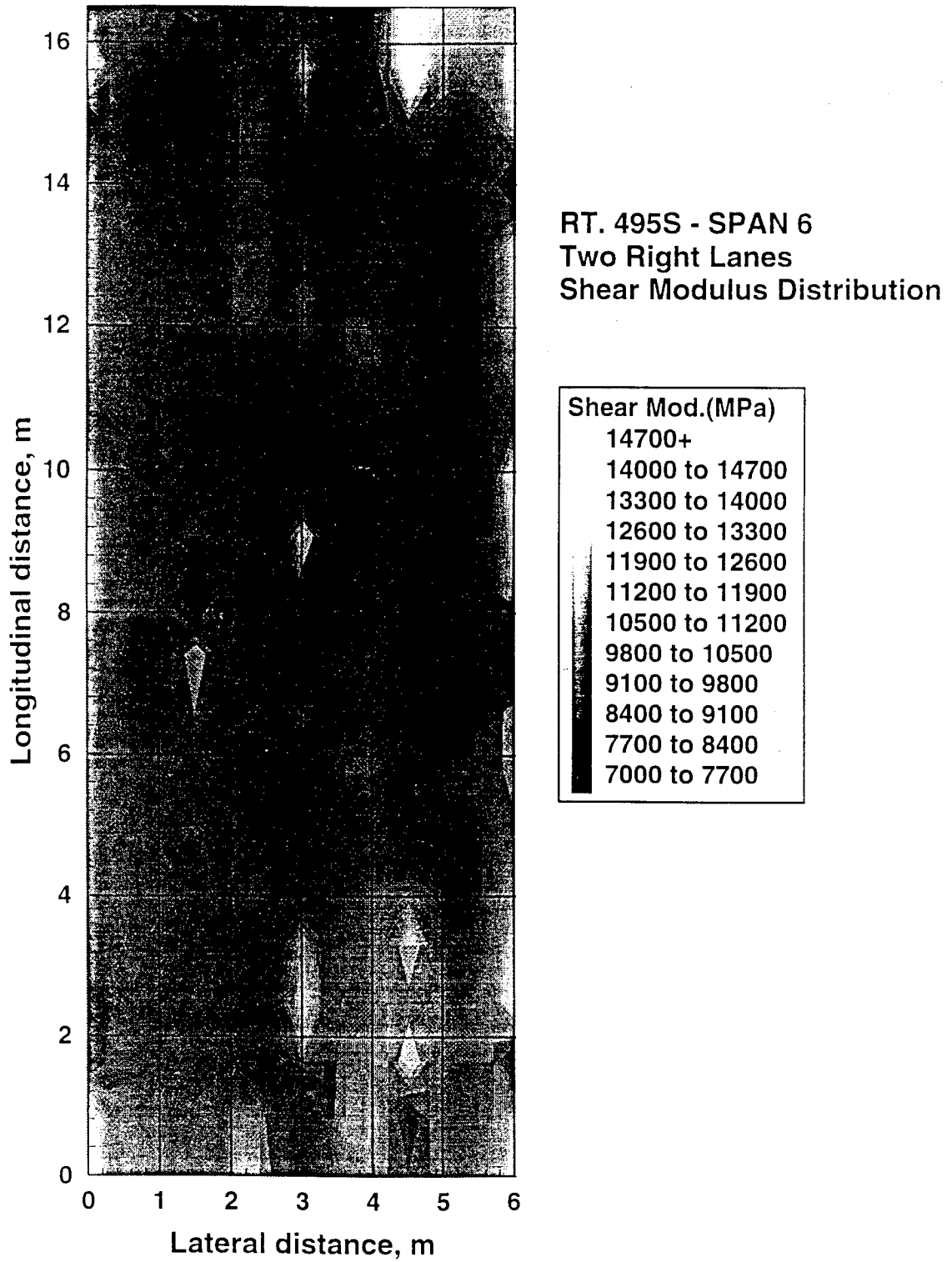


Figure 4.6. Shear modulus distribution for the right two lanes of the 6th span of Rt. I-495S bridge.

m grid, that altogether included about 400 evaluation points. The testing was conducted in May of 1997. Figs. 4.3 to 4.6 include shear modulus and condition assessment distributions for the four lanes tested. As it can be observed from the condition assessment plots, the deck is in a good condition and only small zones of initial delamination can be identified. The PSPA condition assessment data correlate very well with visual observations and results of drag chain examination that identified only a few small areas, almost all in the immediate vicinity of joint mechanisms. Similarly, no significant drops in the elastic properties (shear modulus) can be observed.

Testing on Rt. I-287 over Rt. 1 in Edison, New Jersey

The second example of application of the PSPA device illustrates evaluation of a deck in a significantly deteriorated condition. The evaluation of a bridge on Rt. I-287S over Rt. 1 near Edison, New Jersey, was conducted in August of 1997. The tested deck was about 15 m long, about 21 m wide in the perpendicular direction, and had a skew angle of about 30 degrees. A schematic of the areas of the bridge deck tested are shown in Fig. 4.7. The deck was tested during two 4 hour test sessions, as marked in the deck schematic by Zones A and B. Letters defining test columns and numerals defining test rows for both of the zones are identify positions of all 638 test points.

The condition assessment of the bridge deck is presented in Figs. 4.8 and 4.9. In contrast to the Rt. I-495 bridge deck, zones of all previously described conditions (grades) can be identified in the case of the Rt. I-287S bridge deck. The condition assessment can be presented in continuous and discrete formats, as it is illustrated in the figures. Actual data evaluation and interpretation was done so that

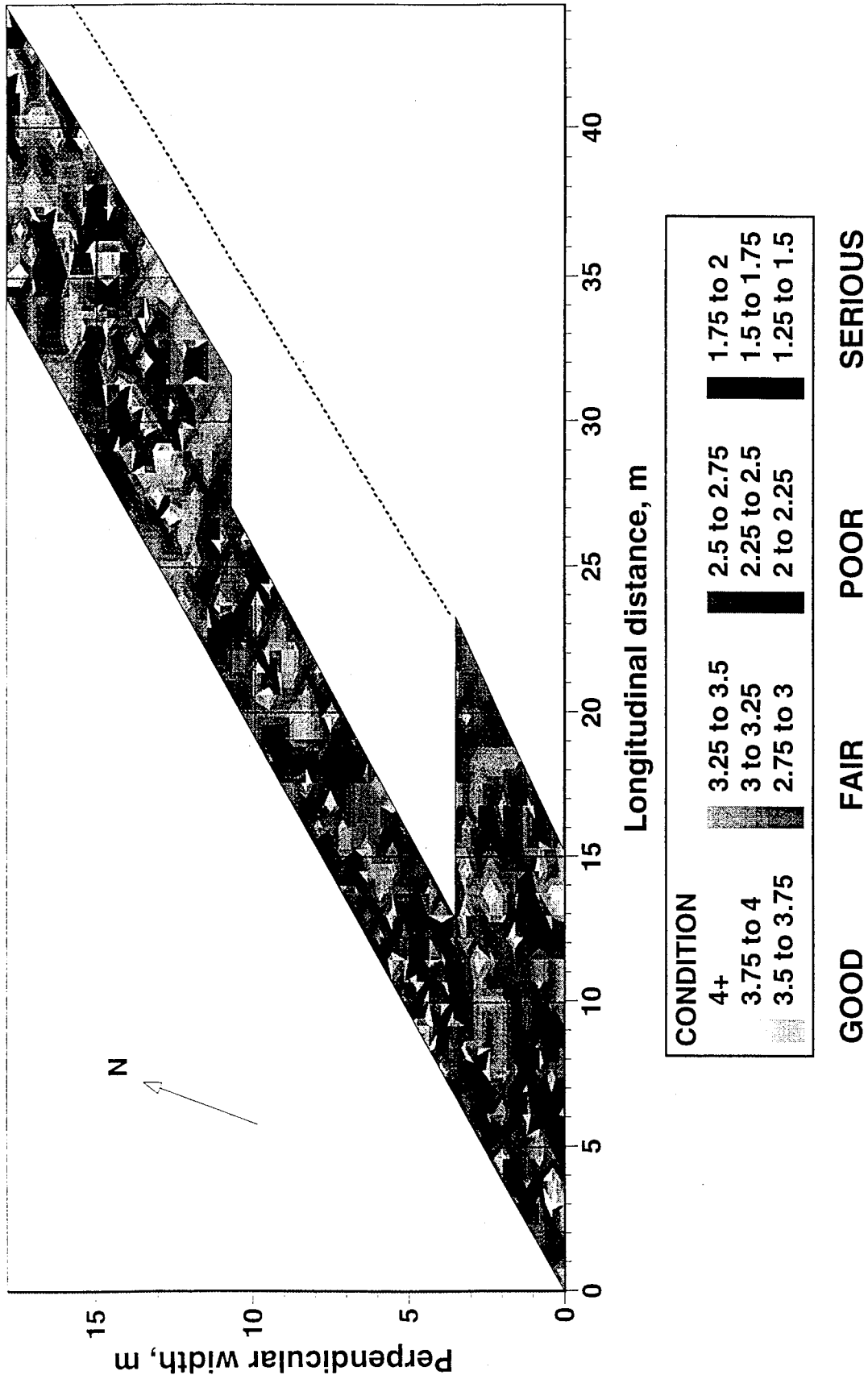


Figure 4.8. Condition assessment of Rt. I-287S bridge deck. Continuous format.

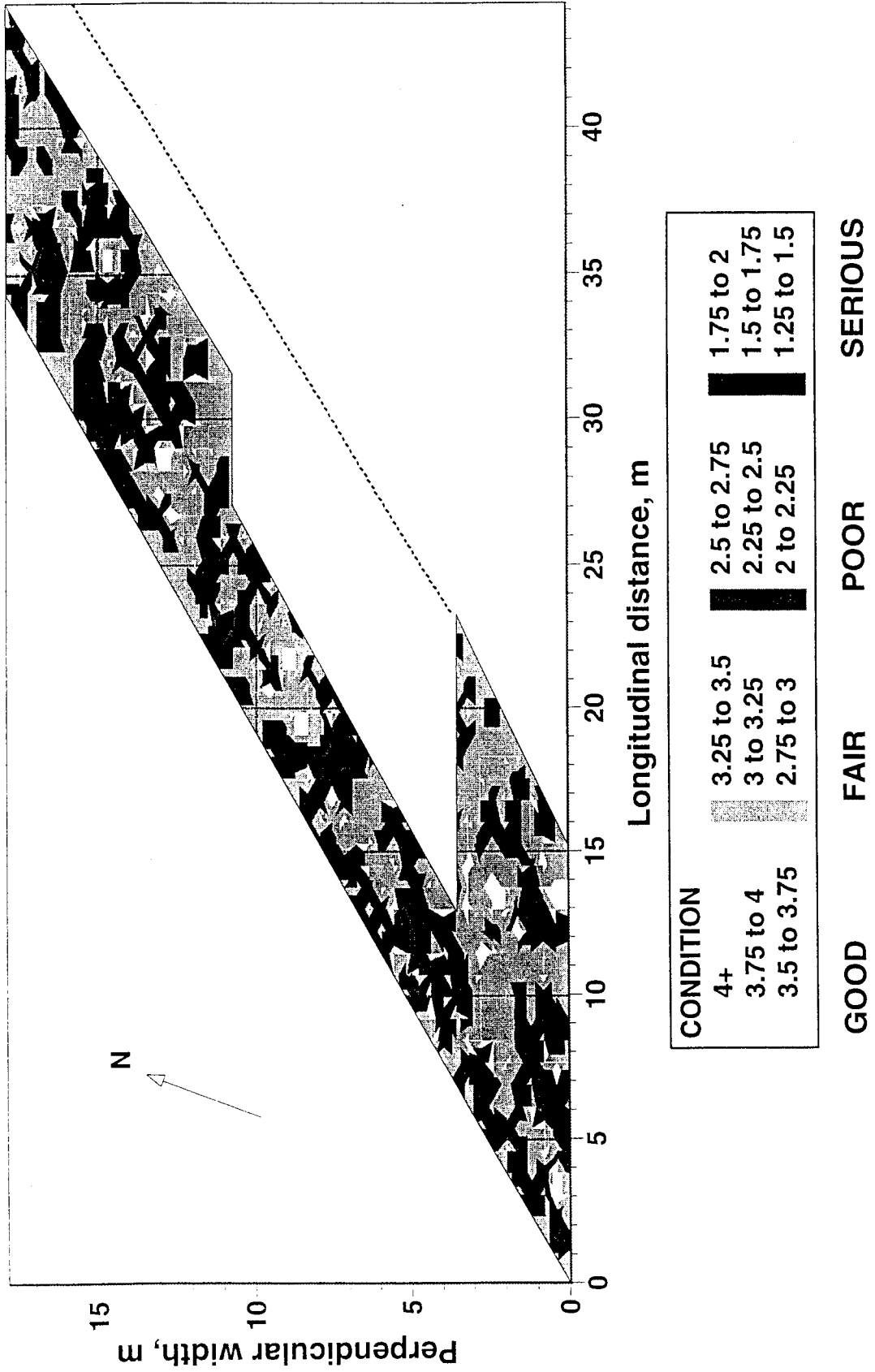


Figure 4.9. Condition assessment of Rt. I-287S bridge deck. Discrete format.

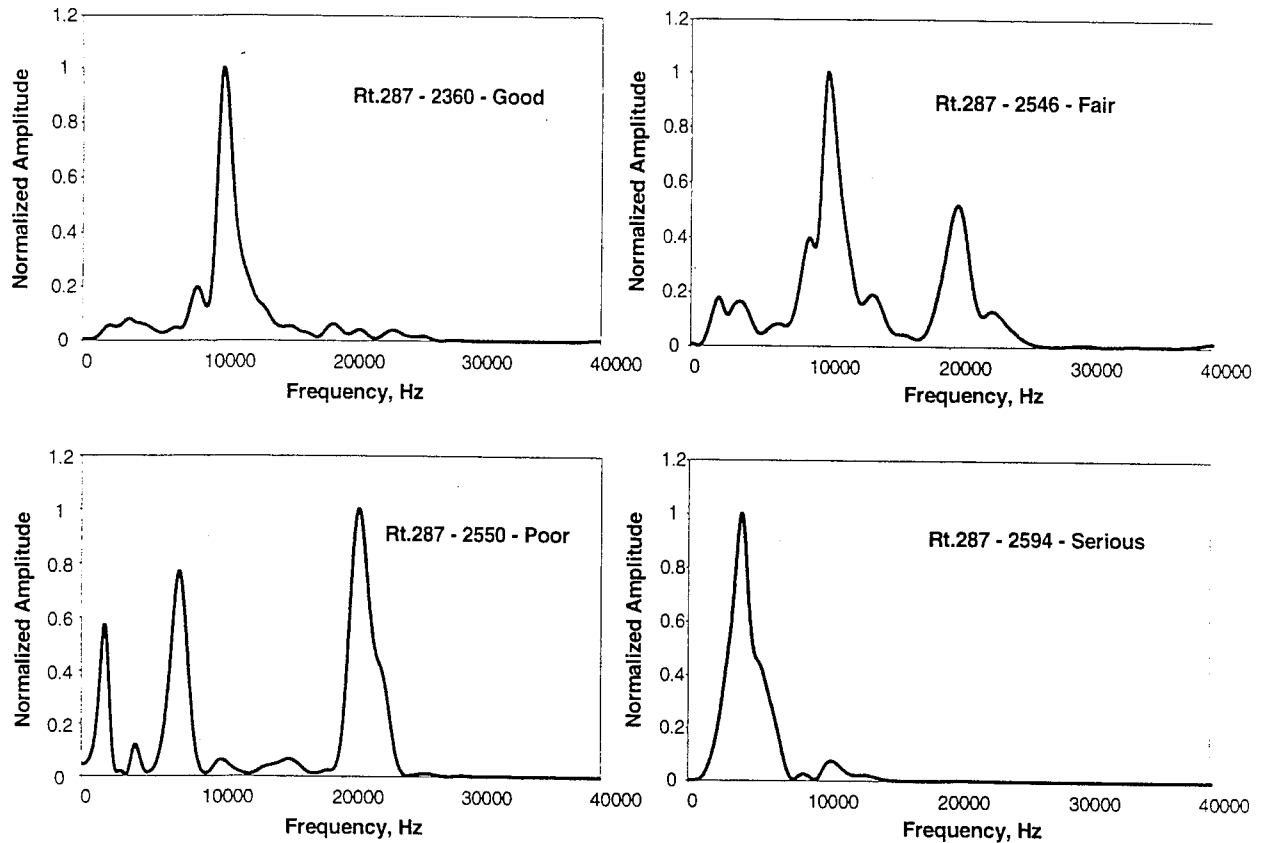


Figure 4.10. Typical spectra for four condition assessment grades.

the thickness of the deck was estimated to be about 17.5 cm or about 7 inches. The return frequency for the full deck thickness is expected to be around 10.5 kHz. Since the position of a delamination is expected to match the top of reinforcement, typically at about the half of the deck thickness, the delamination return frequency is expected to be around 21 kHz. Finally, significant frequency response below the return frequency for the full deck thickness indicates significant contribution of flexural oscillations to the dynamic response.

The bridge deck condition can be presented in terms of grades, as shown in Figs. 4.8 and 4.9, but also in terms of frequency and thickness spectral surfaces for particular bridge deck cross sections.

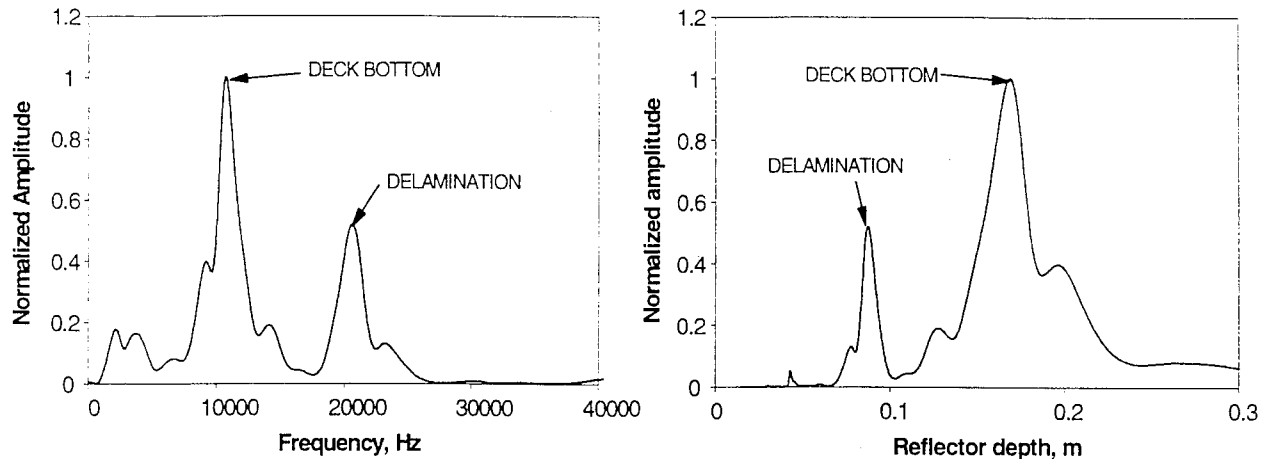


Figure 4.11. Frequency and corresponding thickness spectra for a deck in fair condition.

Such surfaces are formed by presenting spectra for a set of points along a single test line. In the case of a frequency spectral surface, the plot is obtained by simple merging of frequency spectra, like those presented in Fig. 4.10. On the other hand, to form the thickness spectral surface, frequencies need to be converted first into corresponding deck thicknesses. As shown in Fig. 2.5, the depth of the reflector can be described by the ratio of the compression wave velocity and a double return frequency. Therefore, every frequency spectrum can be described by an equivalent thickness spectrum, as illustrated in Fig. 4.11 for the fair condition spectrum from Fig. 4.10. Spectral surfaces for the test line A14-I14 (Fig. 4.13) are presented in Fig. 4.12. High amplitude reflection zones in the frequency spectral surface on the top are described in terms of the position of the reflector and the attributed condition assessment. The reflectors were identified based on a previously approximated return frequency for the full bridge deck thickness, in this particular case around 10.5 kHz. For example, the high frequency zone on the far left side was identified as a delamination. Because no or very little energy was reflected from the deck bottom the condition was described as poor. Smaller low frequency zones point to a possible poor to serious condition. The next zone to

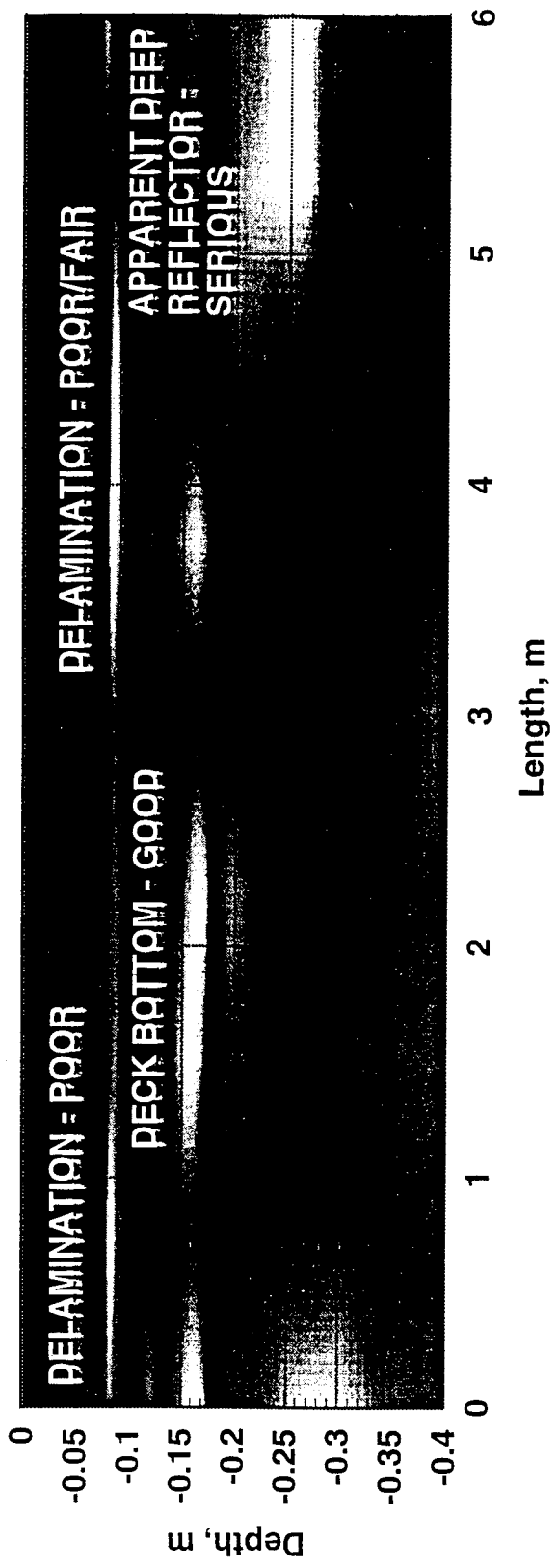
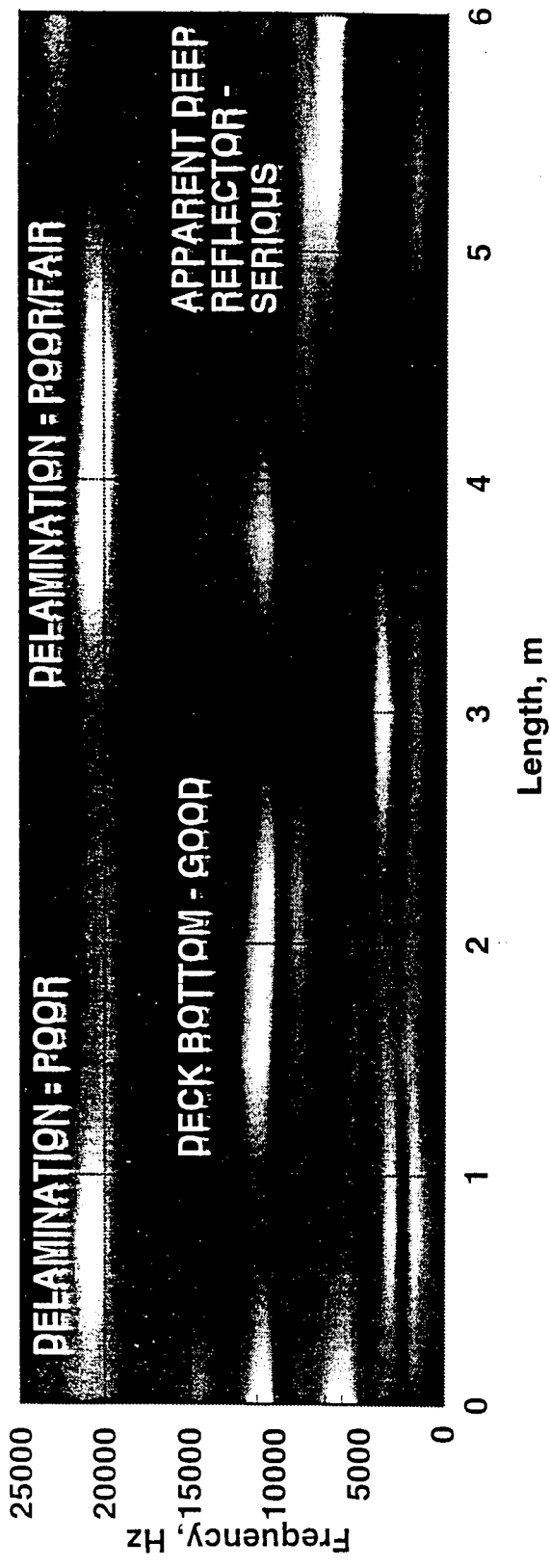


Figure 4.12. Frequency and spectral surfaces for line A14-I14 of Rt. I-287S bridge deck.

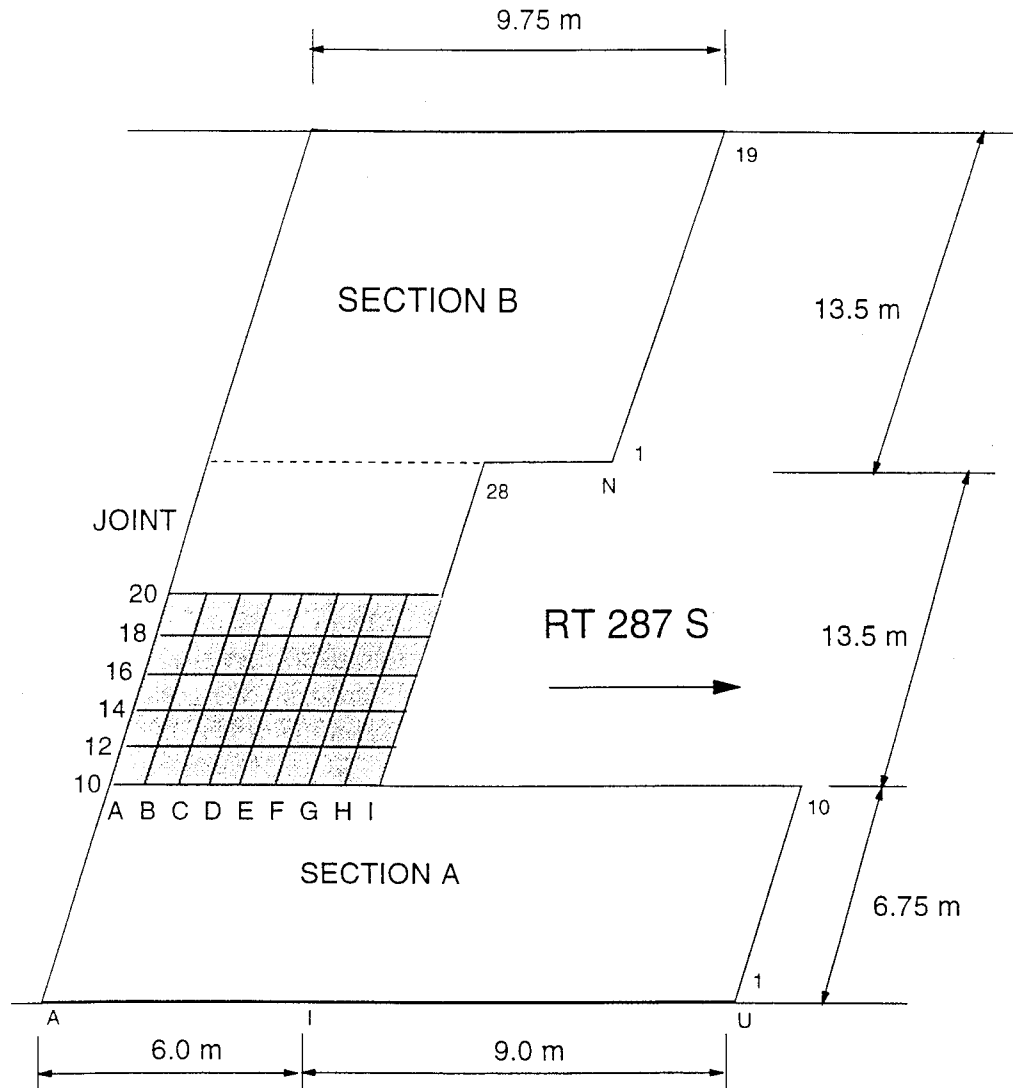


Figure 4.13. Test lines for presented frequency and thickness spectral surfaces.

the right defines clearly a dominant reflection from the deck bottom and consequently a sound condition. The third zone includes again a strong reflection from the probable delamination depth. However, in this particular case a portion of the energy is being reflected from the deck bottom, defining a poor to fair condition. Finally, on the far right side there is a zone of a low return frequency, without significant reflections from either the anticipated delamination elevation or the deck bottom. Such a case is described as an apparent deep reflector and the deck evaluated as in a

serious condition. An equivalent description of the frequency surface is the thickness spectral surface at the bottom. However, an important observation can be made comparing the two surfaces. While the frequency surface provides a better visual detection of delaminations, the thickness spectrum emphasizes the presence of apparent deep reflectors. Certainly, this problem can be corrected by using nonlinear scales for the frequency and thickness axes. Also, attention should be given to the depth range of the thickness spectrum. If the deck is in a serious condition and the response is in a very low frequency range, the apparent depth may be very large and outside the thickness range. An example is the zone between 3 and 5 m, clearly visible in the frequency surface, but outside the range of the thickness spectrum. Several thickness spectral surfaces for six test lines defined in Fig. 4.13 are presented in Figs. 4.14 and 4.15.

Parallel to the PSPA testing, the bridge deck was evaluated by a chain dragging procedure. The comparison of the condition assessment results obtained from the PSPA testing and the deteriorated zones determined by the chain drag are compared in Fig. 4.16. The comparison points to a similarity of the two approaches in detection of areas with progressed delamination (poor to serious condition). The ability of the chain drag to identify zones in a serious condition can be explained by the fact that the frequency response in such cases is within the audible range, in this case typically between 2 and 7 kHz. On the other hand, most of the zones identified by the PSPA as zones of initial delamination (fair to poor grades) were not detected by the chain drag. As illustrated in the previous spectra and spectral surfaces plots, the return frequency for reflections from the delamination is above 20 kHz, outside the audible range. This ability of the PSPA device to detect signs of initial delamination represents a significant advantage of the device's ultrasonic testing over the chain drag approach. It

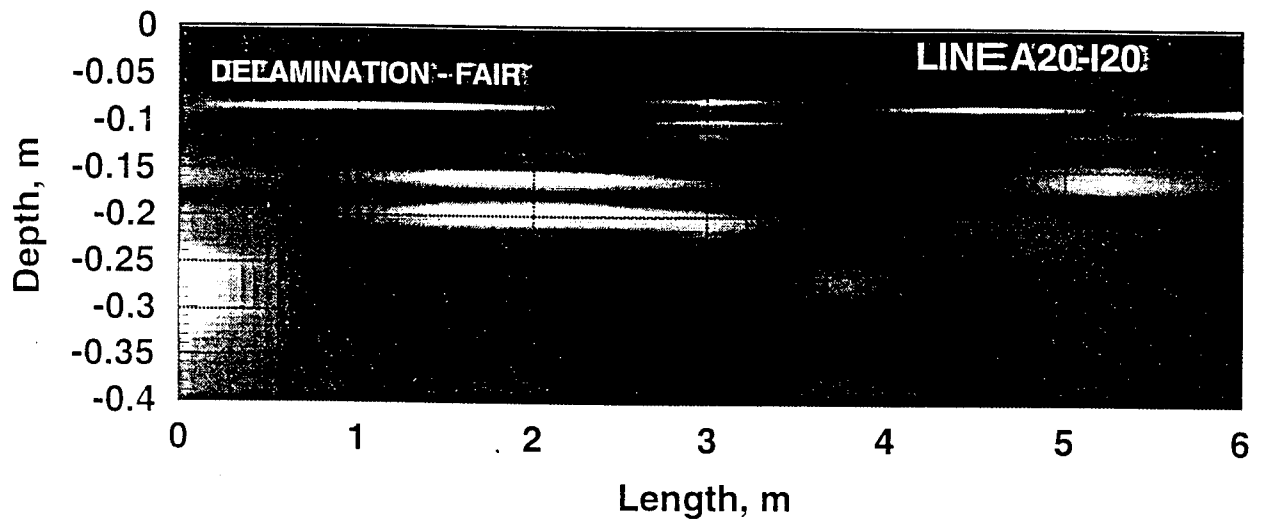
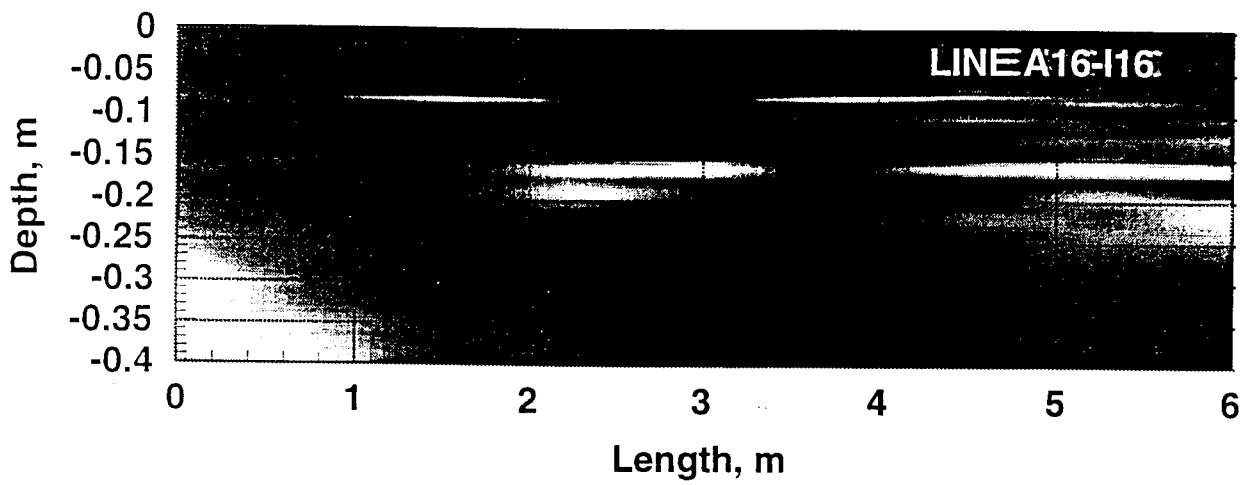
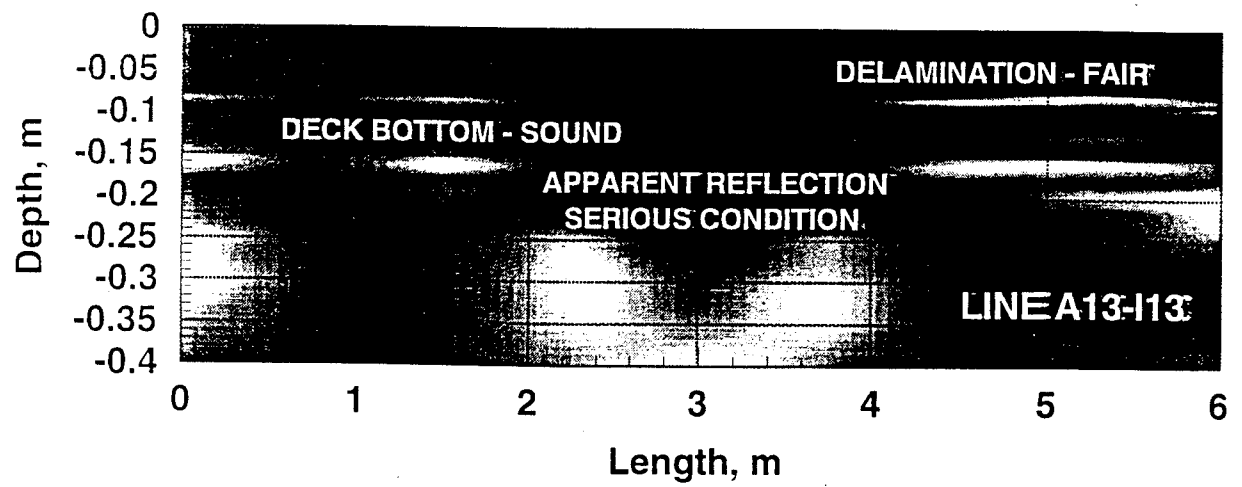


Figure 4.14. Thickness spectral surface for sections A13-I13, A16-I16 and A20-I20.

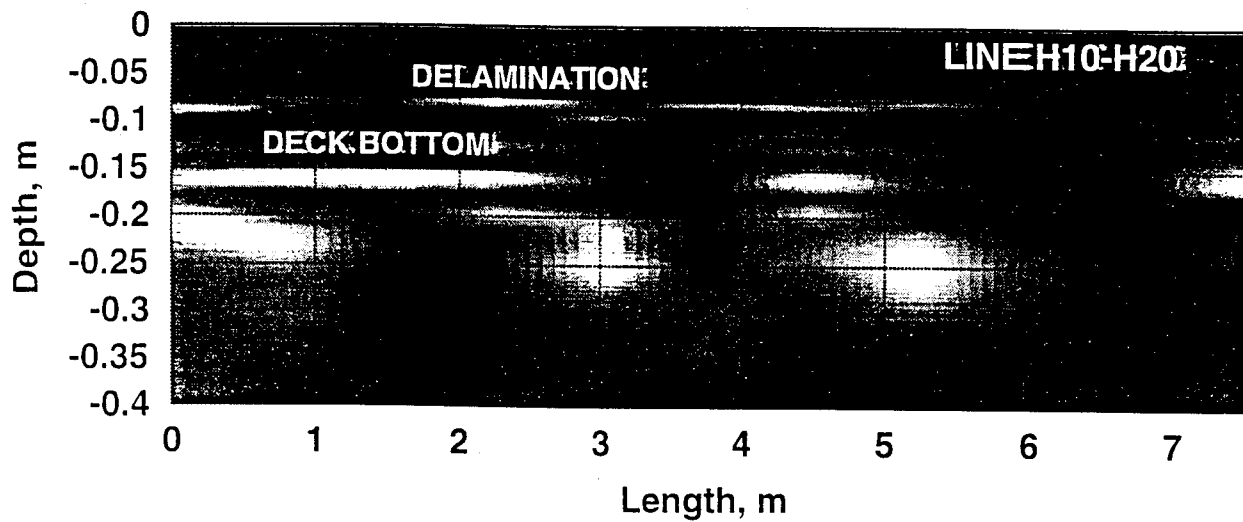
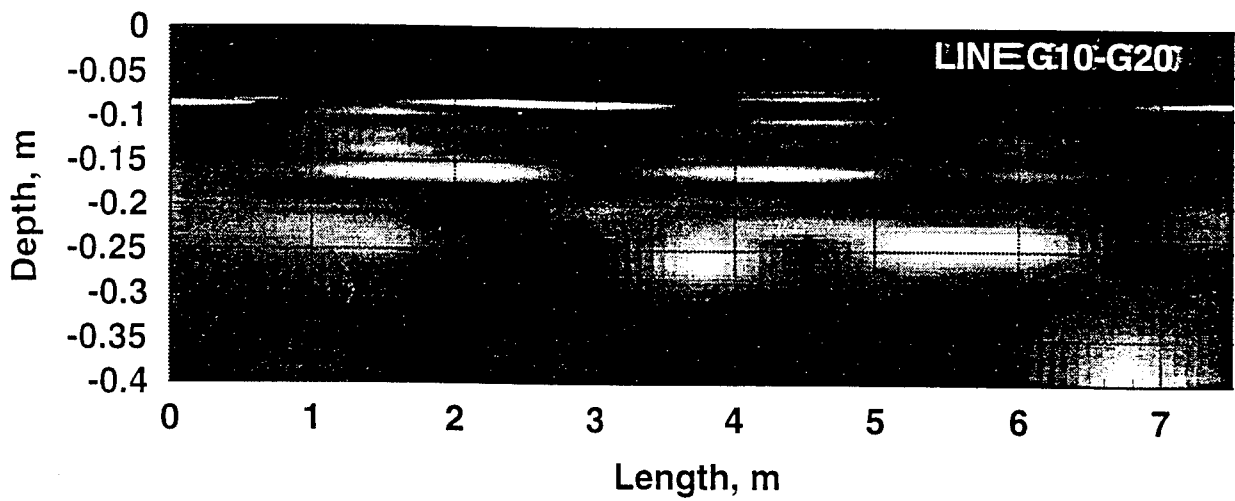
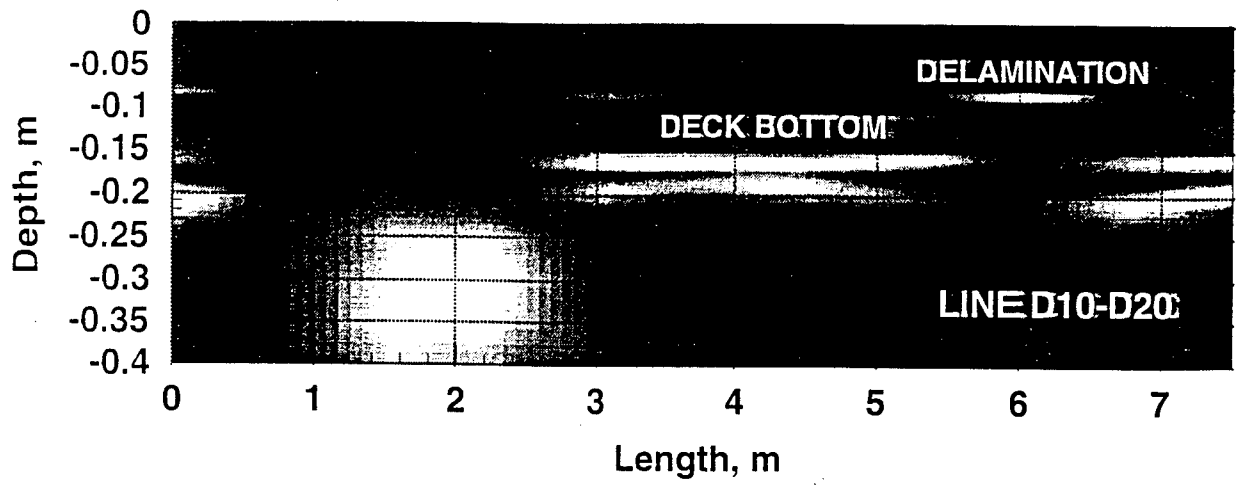


Figure 4.15. Thickness spectral surfaces for sections D10-D20, G10-G20 and H10-H20.

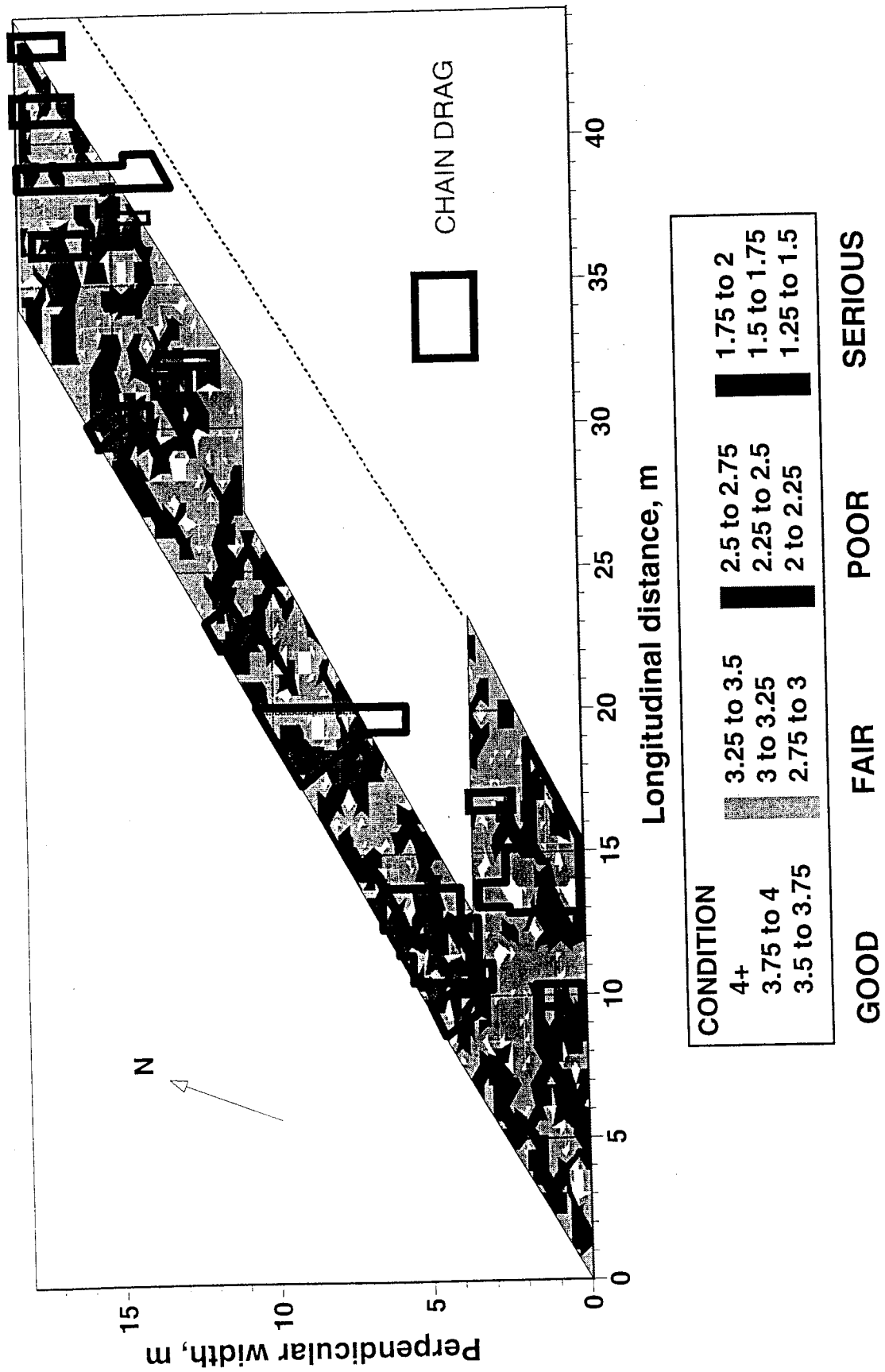


Figure 4.16. Comparison of PSPA and chain drag condition assessment for a section of Rt. 1-287S bridge deck.

allows a better prediction of delamination progression, because it can be evaluated at all of its stages, from initial to progressed and widely separated deck layers. The ability to detect early signs of deck delamination can lead to better assessment and timing for implementation of rehabilitation measures, and thus more economical management.

CHAPTER 5

NUMERICAL SIMULATION OF SEISMIC TESTING ON BRIDGE DECKS

Evaluation of bridge decks by seismic methods, and the PSPA device, was simulated for three purposes. The first purpose was to quantify the relationship between the size and severity of a delamination and the frequency spectrum content obtained from the impact echo test, thus to minimize subjectivity in the definition of the deterioration degree. The second purpose was to evaluate limitations of seismic methods and the PSPA device in delamination detection. Finally, the third purpose of numerical simulations was to simulate hypothetical deterioration processes in a bridge deck that lead to significant and detectable delaminations. The last task was conducted for the purpose of evaluation of the capability of seismic methods to assist in long term monitoring of delamination progression processes. All the simulations were conducted using the finite element program ABAQUS. The following sections include a description of the finite element model and results of a parametric study conducted.

Finite Element Model

Simulation of seismic testing on a bridge deck is done on an axisymmetric model of a deck of a 2.5 m radius and a 25 cm thickness. Five model discretizations were examined, as shown in Fig. 5.1. Model 1 involves discretization of the deck using 2.5x2.5 cm 8-node biquadratic axisymmetric elements. Model 2 is identical to Model 1 except that discretization in the vicinity of the axis of symmetry (impact source location), of a radius of 12.5 cm and 15 cm deep, is done by 1.25x1.25 cm

8-node biquadratic elements. As described and illustrated later, the primary purpose of a finer discretization in vicinity of the axis of symmetry was to minimize effects of artificially amplified surface wave components. Model 3 is discretized entirely by 1.25x1.25 cm elements. Finally, Models 4 and 5 are identical to Model 2, except that discretization in vicinity of the source is done by circular meshing in Model 4, and by a combination of square and circular meshing in Model 5. In all models concrete is described as having a shear wave velocity of 2000 m/s, compression wave velocity of 3260 m/s (Poisson's ratio of 0.2), and mass density of 2500 kg/m³. Damping is described as Rayleigh damping, with parameters α equal to 0 and β equal to 10⁻⁵. Delaminations are described as cracks, defined by two sets of elements connected along the crack to two mutually independent sets of points. Other basic geometrical properties of a delamination include depth d and radius R , as depicted in Fig. 5.1.

The impact is described so to closely simulate impact echo testing using the PSPA device. A description of the impact in terms of trapezoidal and haversine functions of a 50 μ s duration is used. A time integration scheme using 1024 constant 2 μ s time increments (identical to the PSPA sampling) is implemented, providing a Nyquist frequency of 250 kHz and approximately a 500 Hz frequency resolution. A typical frequency range of interest for bridge decks of a thickness of 20 to 30 cm is 5 to 30 kHz, where the lower frequency range of 5 to 10 kHz corresponds to reflections from the deck bottom, and the upper frequency range to reflections from delaminations. The 2 μ s time increment used ensures that wave propagation distance during a single time increment is less than a length of a single finite element. Displacement, velocity and acceleration histories were obtained at all surface points less than 60 cm away from the source. Because the compression waves

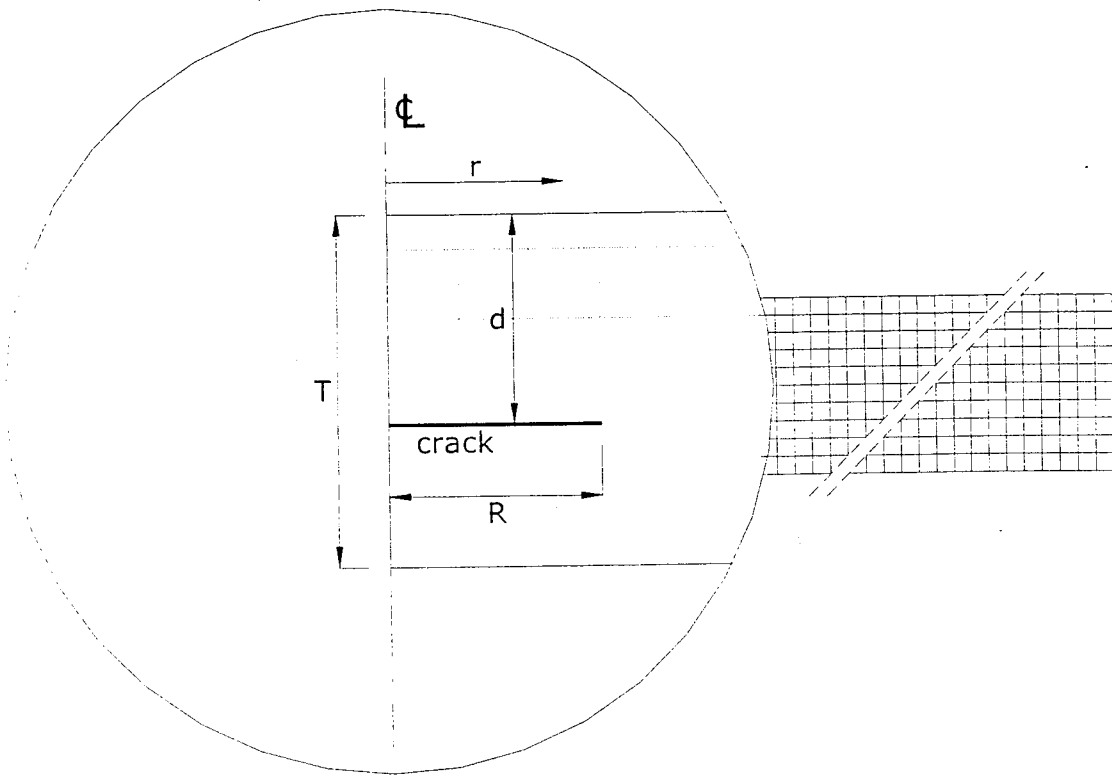
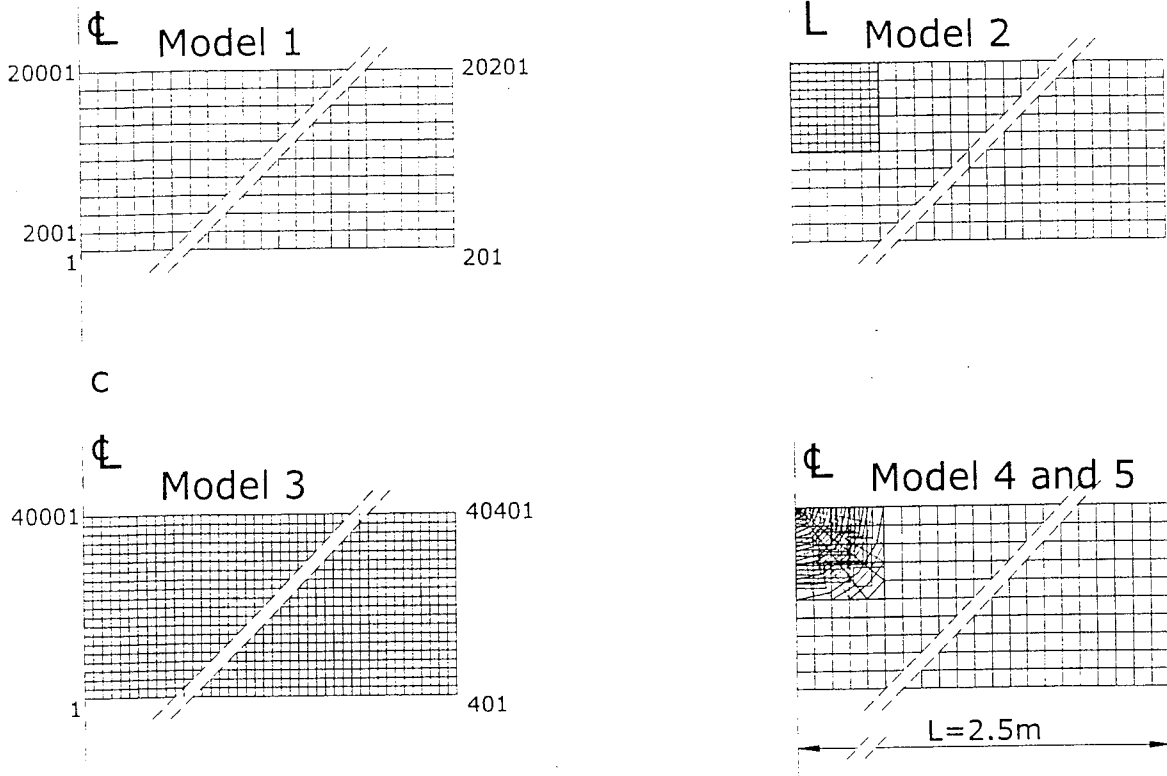


Figure 5.1. Finite element models used in simulation of PSPA testing.

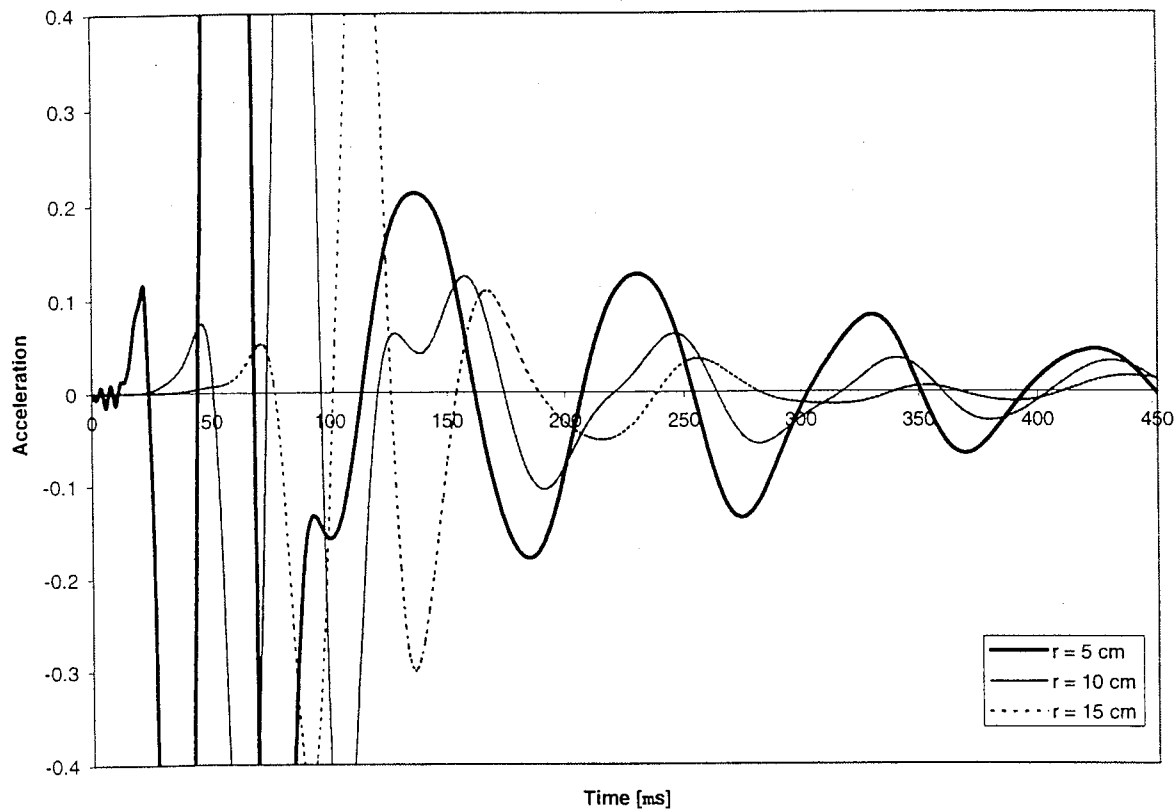


Figure 5.2. Typical acceleration histories for three receiver locations, $T=25$ cm, $d=15$ cm, $R=15$ cm.

being reflected from the deck bottom and delaminations have a dominant vertical component, the PSPA utilizes vertically oriented accelerometers. Therefore, vertical acceleration histories were also of primary interest for this study. Typical acceleration histories at radial distances of 5, 10 and 15 cm from the source, due to a haversine impact function, are shown in Fig. 5.2. The shape of a 15 cm acceleration history matches well a form of a signal typically obtained in the field, with distinctive compression, shear and surface wave components.

For receiver positions close to the impact source, for example for the 5 cm near receiver distance history in Fig. 5.2, irregularities in the acceleration history caused by the discretization near the axis

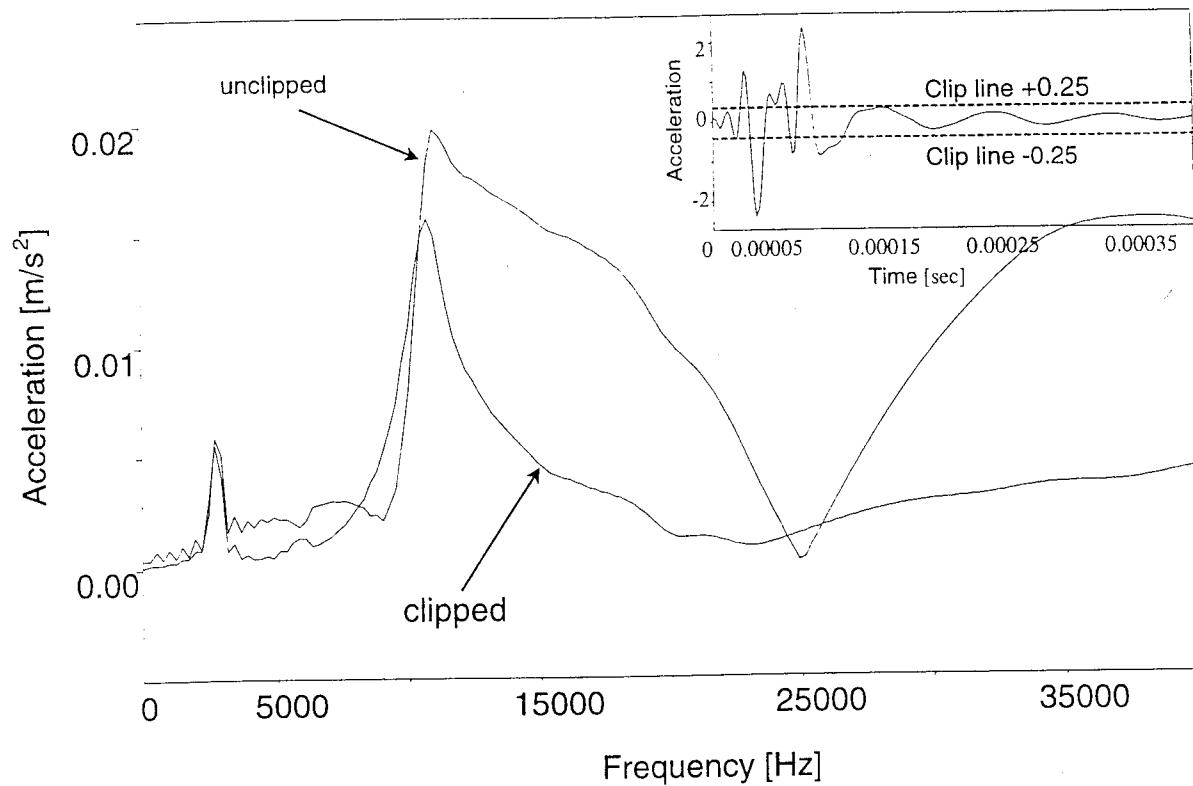


Figure 5.3. Effect of clipping of surface waves on spectra. $T=25$ cm, $d=15$ cm, $R=15$ cm, $r=7.5$ cm.

of symmetry can be observed. A very low elemental stiffness near the axis of symmetry (Zienkiewicz and Taylor, 1989; Hughes, 1987) causes generation of artificially high surface wave components in its vicinity. This problem was also reported by Sansalone and Street (1997). An efficient way to reduce effects of these surface wave components, but at the same time to preserve a portion of a signal describing compression wave reflections, is to clip time histories in the surface wave portion. This is illustrated in Fig. 5.3 for a deck with a 15 cm deep delamination, of a 15 cm radius. The response spectrum of an unclipped signal calculated at a 7.5 cm distance from the source provides a spectrum with a barely recognizable return frequency, which in this case should be about 10.8 kHz. On the other hand the return frequency peak for a clipped signal can be well distinguished and

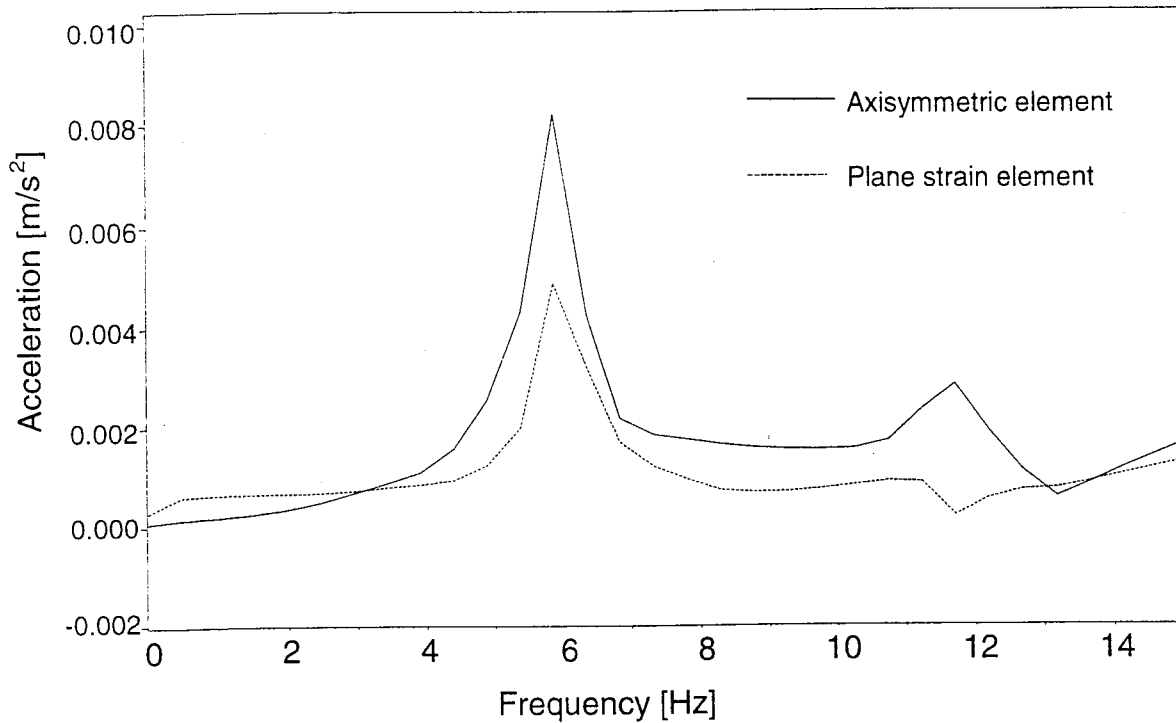


Figure 5.4. Comparison of response spectra obtained from axisymmetric and plane strain models.

resembles those obtained in actual field testing. To confirm the effect of a reduced stiffness of axisymmetric elements in vicinity of the axis of symmetry, results were compared to those for a plane strain model. As illustrated in Fig. 5.4, the response spectrum for an unclipped history for the plane strain model matches well the spectrum of the clipped history for the axisymmetric model.

Effect of Receiver Positioning, Impact Source Function and Delamination Geometry

The effect of receiver positioning on IE response spectra was investigated first. The effect of the parameter was investigated for an assumption that the impact source is above the midpoint of a delamination. As illustrated in Fig. 5.5 for a deck with a delamination 15 cm deep and of a 15 cm

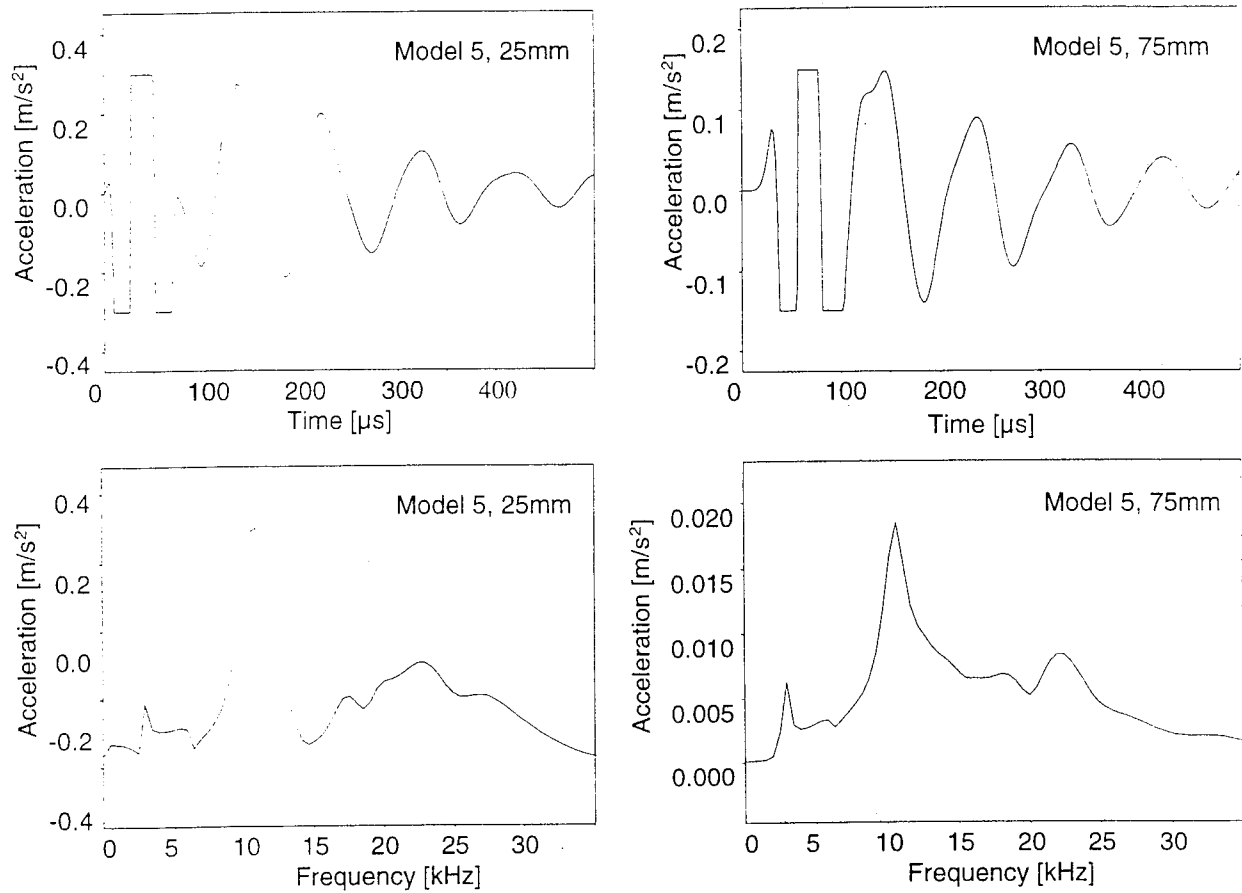


Figure 5.5. Comparison of clipped time records and time spectra for 25 and 75 mm receiver positions.

radius, and for a haversine impact function, the return frequency peak can be clearly identified for both 25 and 75 mm distances from the source. It is also obvious, that the peak distinction decreases with the distance from the source. Other results, not presented herein, demonstrate that the return frequency peak is distinguishable for receiver positions less or equal to the delamination radius.

As described earlier, the most important objective of using several finite element models was to minimize effects of artificially strong surface waves. To attempt the same, a relatively “rough” trapezoidal impact function was substituted by a “smooth” haversine function. A comparison of time records for two extreme conditions in Fig. 5.6, Model1 with a trapezoidal and Model 5 with a

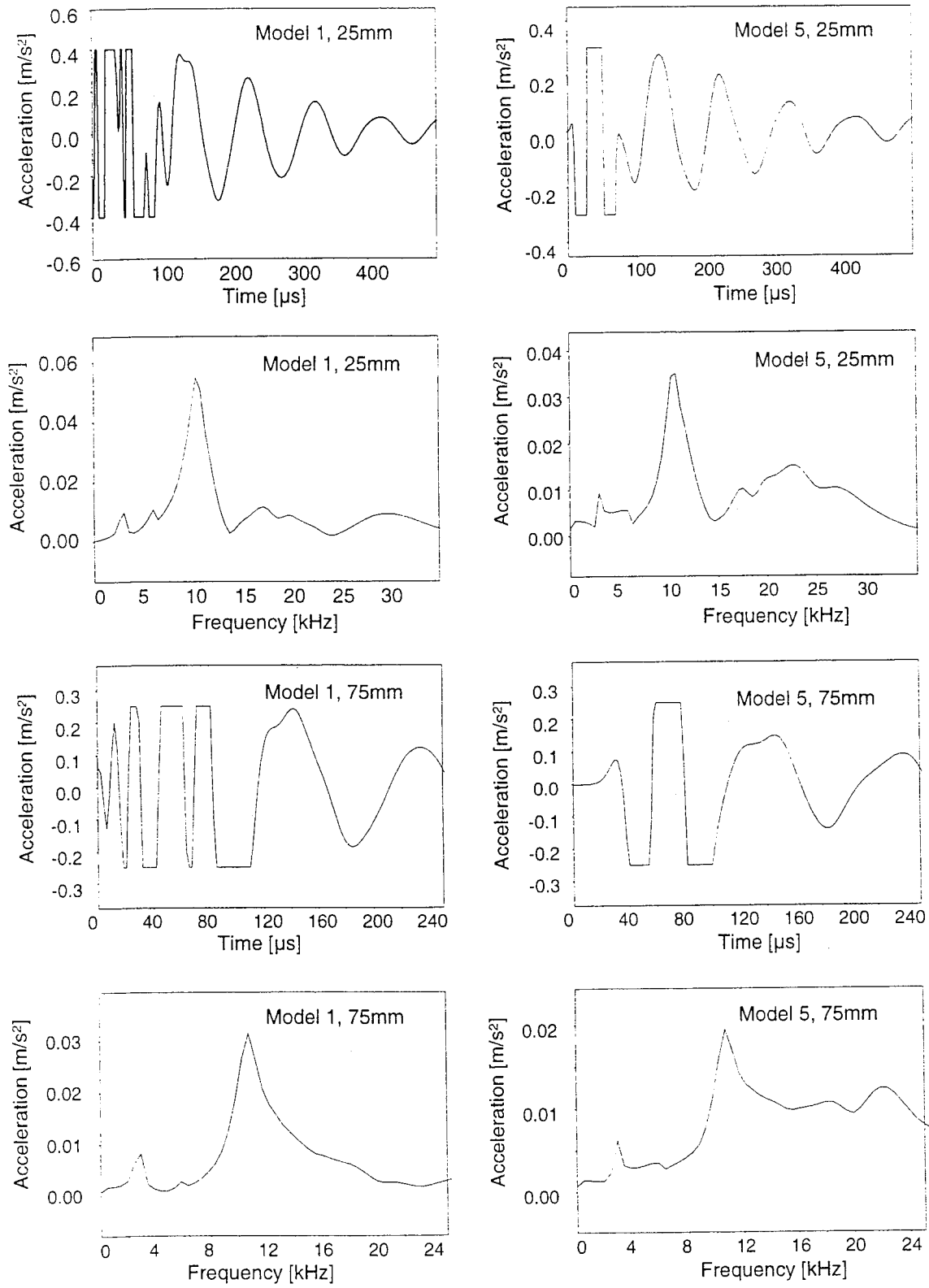


Figure 5.6. Comparison of time records and spectra for Model 1 with trapezoidal loading and Model 5 with haversine loading at radial distances fo 25 and 75 mm.

haversine loading, indicates a clear improvement in the reduction of surface wave components for Model 5. Surprisingly, the return frequency for Model 1 is equally well, if not better, pronounced. In general, while the spectra for five models and two loading functions differ somewhat, they define equally well and almost identical return frequency. It may be concluded that, while the model discretization and the impact source description are critical in the description of wave propagation histories in vicinity of the source, they have little effect on the simulation of the IE test spectrum. The effect of the vertical position of a delamination is illustrated in Fig. 5.7. From the pointed return frequency values of 7580, 10880 and 16760 Hz, and the compression wave velocity of 3260 m/s, delamination depths of 21.3, 15.3 and 10.3 cm, respectively, can be determined. This confirms the ability of the IE technique to precisely define the delamination depth. Similarly, very little

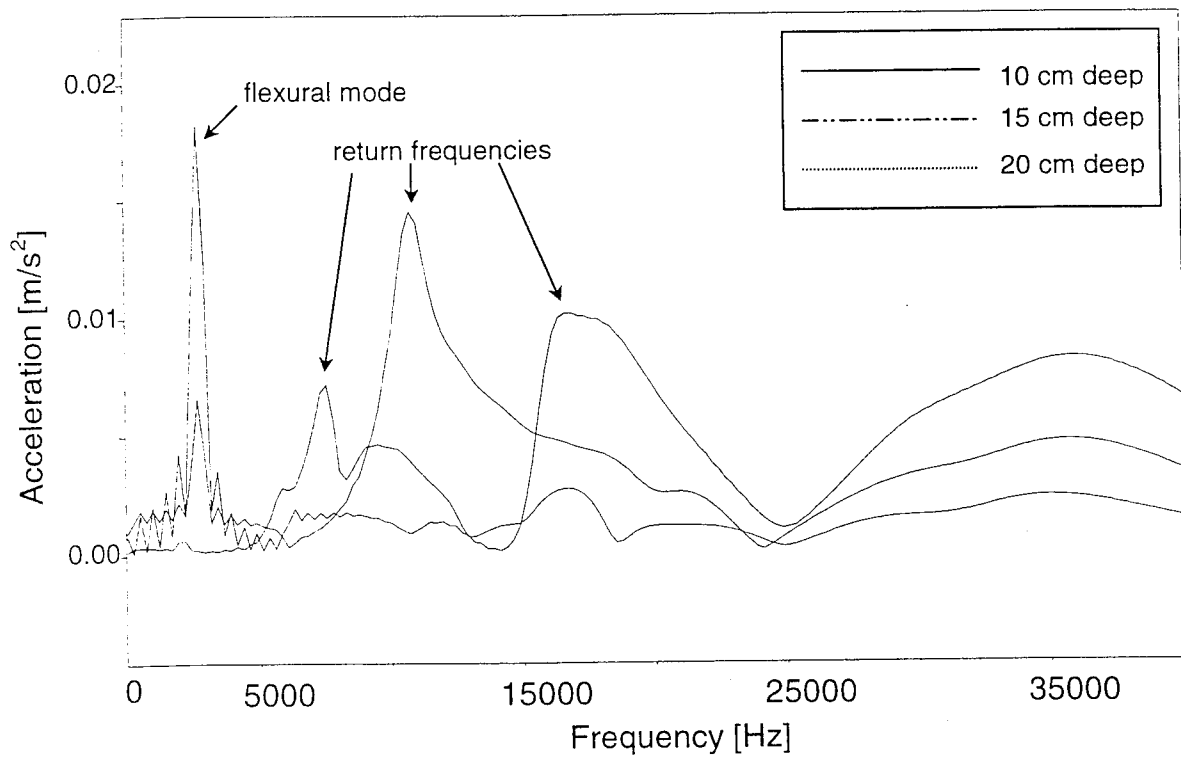


Figure 5.7. Effect of the delamination position on spectra. $T=25\text{cm}$, $R=15\text{cm}$, $r=7.5\text{cm}$.

differences in the return frequency were observed (not shown herein) for a variation of the delamination radius between 15 and 60 cm. This is in agreement with previous findings by Sansalone (1993) that the response for a deck with a delamination of a radius larger than about 0.75 of the delamination depth corresponds to the response for a sound deck of a thickness equal to the delamination depth. As the delamination depth decreases, while the delamination radius is kept constant, flexural oscillations of the upper portion of the deck get more pronounced. This can be observed in Fig. 5.7 for delamination depths of 10 and 15 cm. Based on the presented and other developed spectra, it can be concluded that the flexural mode peak becomes visible for delamination depth to radius ratios less or equal to about 1. The conclusion is valid for an assumption, as modeled herein, that the source is at the center of the delamination and that the receiver is within the projected borders of the delamination.

Simulation of Delamination Progression

It is assumed that the deck condition worsens according to two probable delamination progression scenarios. The first scenario involves expansion\growth of a single small delamination, while the second one involves progressive linking of several smaller delaminations. The first scenario is illustrated in Fig. 5.8 by response spectra for delaminations of a radius varying from 2.5 to 15 cm, and for a delamination depth of 15 cm. Again, the receiver is placed at a 7.5 cm radial distance from the source. For a small radius, 2.5 and 5 cm, the return frequency peak for the delamination is very weakly defined. As the radius increases, the delamination peak dominates the spectrum. On the other hand, a transition of the full deck thickness peak towards the flexural mode

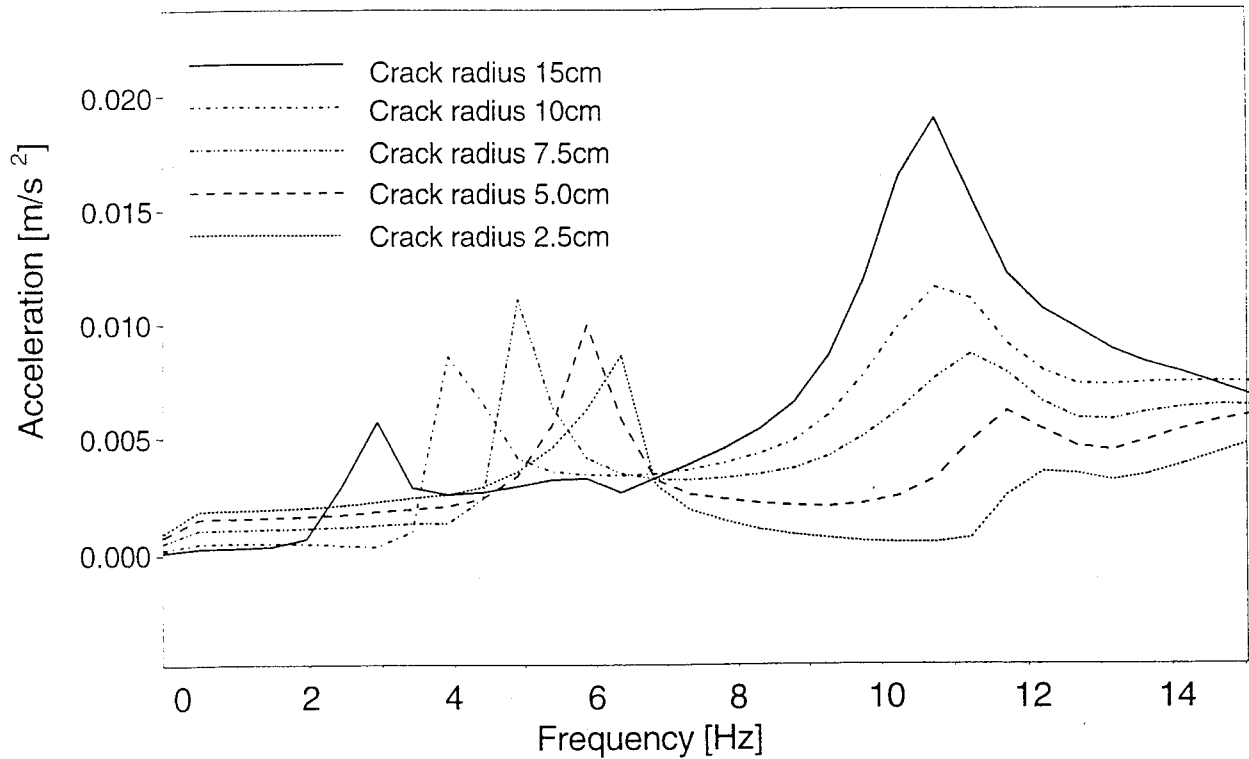


Figure 5.8. Scenario 1. Changes in the response spectrum due to delamination expansion.

peak can be observed as the delamination radius increases. Similar observations (not presented herein) are valid for receiver positions closer to the source, for example for 2.5 and 5.0 cm. For receiver positions approaching or greater than the radius of the largest delamination, the transition of the full deck thickness peak towards the flexural mode peak is preserved, while the delamination peak becomes barely visible. Previous observations point to a conclusion that the growth of a delamination can be recognized in periodic monitoring results through two elements. The first one is a growth of the delamination return frequency peak, and the second one a shift of the full deck thickness peak towards a lower frequency flexible mode peak.

The second scenario of progressive linking of several smaller delaminations is illustrated in Figs. 5.9

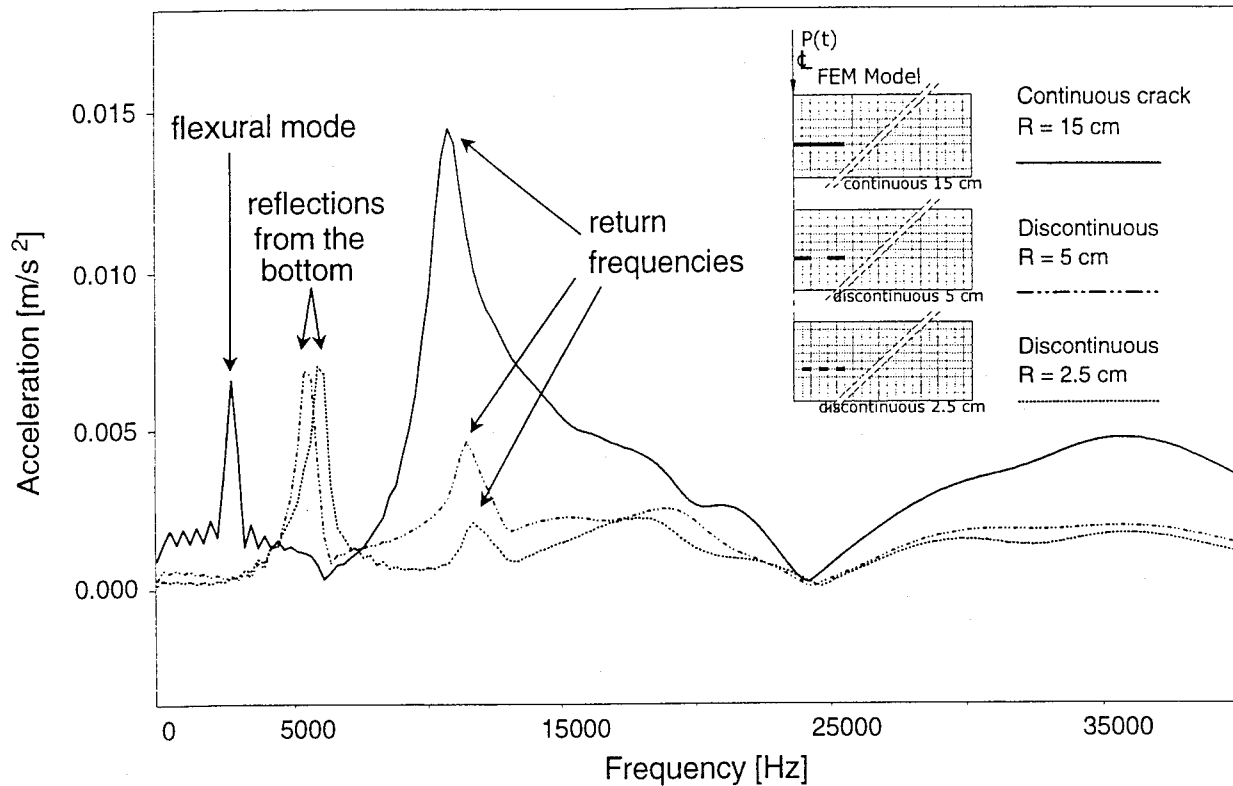


Figure 5.9. Scenario 2. Changes in the response spectrum due to progressive linking. $T=25$ cm, $d=15$ cm, $R=15$ cm, $r=7.5$ cm.

and 5.10. Three cases are compared in Fig. 5.9: a continuous delamination of a 15 cm radius, a discontinuous 15 cm circular delamination with a 5 cm contact ring in the middle, and a discontinuous 15 cm circular delamination with three 2.5 cm wide contact rings. In all three cases the return frequency can be identified, however the peak gets weaker as the frequency of contact areas increases. While the flexural mode for the continuous delamination is clearly visible, it does not exist for the other two. Finally, peaks left from the delamination return frequency for the discontinuous delamination models can be observed. These peaks correspond to reflections from the bottom of the deck, confirming expected partial radiation of energy towards the bottom of the deck through the periodical contacts. Similar results are obtained for uneven delamination-contact ring widths, as illustrated by a comparison of spectra for four cases of continuity in Fig. 5.10. The 15 cm

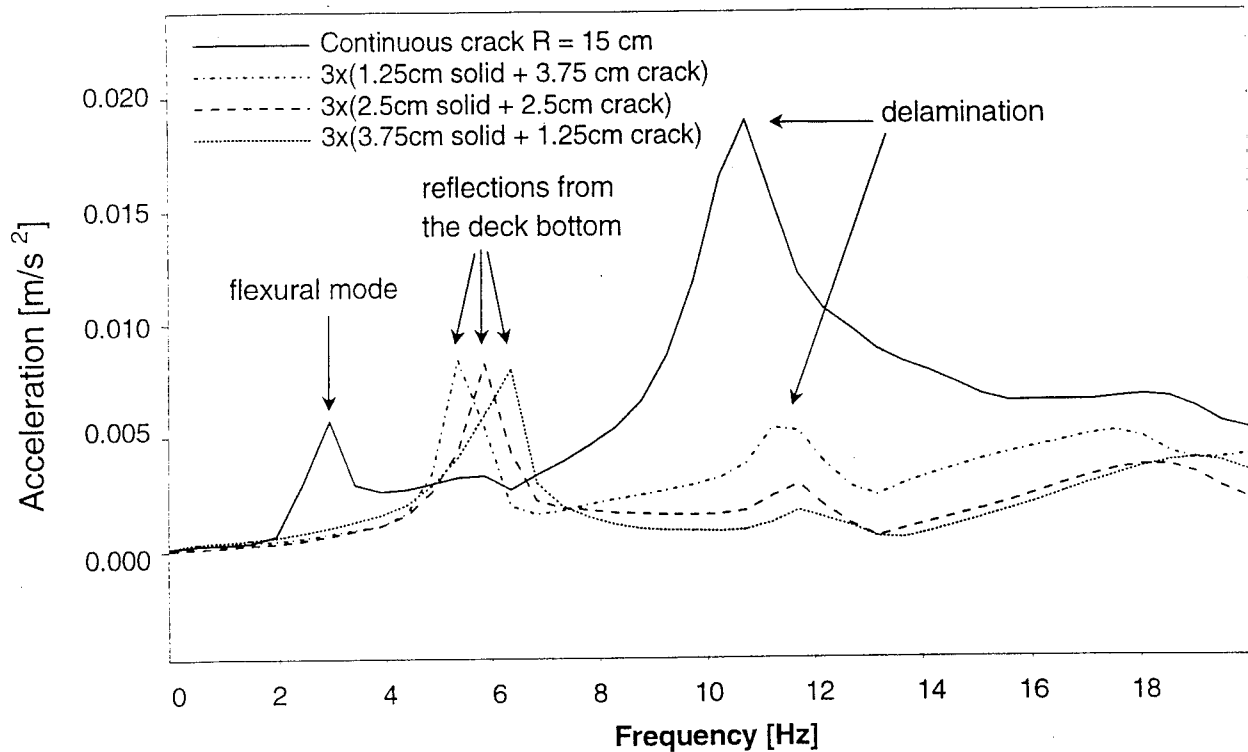


Figure 5.10. Scenario 2. Changes in the response spectrum due to progressive linking. $T=25$ cm, $d=15$ cm.

radius delamination cases include: a continuous delamination, a discontinuous delamination of three intermittent 1.25 cm contact and 3.75 cm crack ring widths, starting from the center, and discontinuous delaminations of three intermittent 2.5 cm contact and 2.5 cm crack, and 3.75 cm contact and 1.25 crack ring widths.

While there are some similarities between the two scenarios, the most important difference from the long term monitoring point is in the transition from the full deck thickness return frequency peak towards the flexural mode peak. In the crack expansion case the transition is gradual, while in the crack linking case that transition is sudden and happens when the delamination becomes continuous.

CHAPTER 6

DATA VISUALIZATION

In addition to an accurate condition assessment, an important aspect of bridge deck evaluation includes fast and simple data presentation and interpretation. A 3-dimensional, real time, presentation of evaluated sections of a bridge deck seems to be a logical solution to the task. Therefore, a program is being developed that provides 3-dimensional mapping of the recorded impact echo data, as illustrated in Fig. 6.1. The objective of the program is to define zones of high

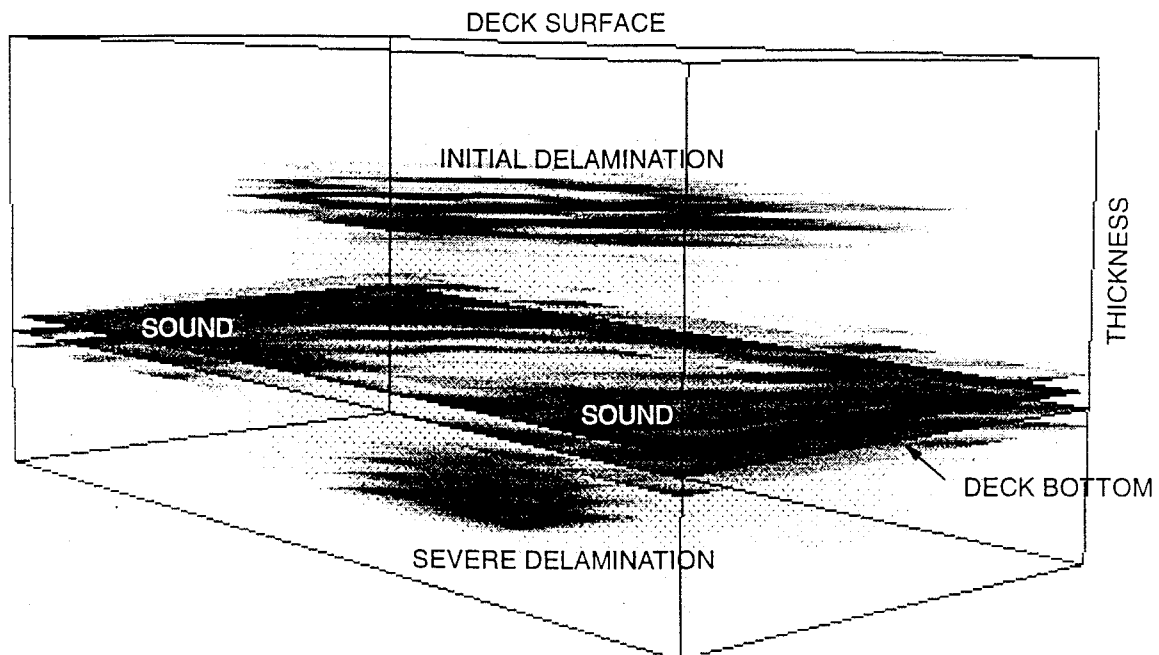


Figure 6.1. 3-dimensional thickness spectrum for a bridge deck section.

intensity reflections and present them in a translucent 3-dimensional model of a tested deck section. Figure 6.1 was generated using synthetic data for the purpose of illustration of previously described possible deck conditions and corresponding grades. As discussed in Chapter 5, the depth of the reflector can be easily calculated from the known compression wave velocity and the return frequency. The image in the figure contains a 3-dimensional thickness spectrum with lines defining the surface and bottom of the deck. Reflections in a plane matching the deck bottom line define sound zones of the deck. Reflections at about a half deck thickness define delaminated zones. Depending on other reflections below the delaminated zones the condition is described as fair, poor or serious. For example, reflections from the deck bottom can be observed below the edges of the delaminated zone. This is an indication of an initial delamination, or a fair condition. Closer to the center of the delamination, reflections from the deck bottom are very weak. This can be described as a progressed delamination, or a poor condition. Finally, below the very center of the delamination there is a reflection below the deck bottom. As previously explained, this apparent reflection defines a zone of complete and wide separation of deck layers, warning about a serious condition.

The program was implemented on actual data from Rt. I-287S bridge testing. Figures 6.2 and 6.3 illustrate implementation of the program on the deck section marked in Fig. 4.13. For the simplicity, in this case the deck section was described as a rectangular instead of a skewed section. As in Fig 6.1, zones of a sound deck and of initial, progressed and complete delaminations can identified from reflections at various deck elevations. The current effort is being directed towards implementation/linking with existing PSPA software that will allow such a presentation in a real time. Once completed, the PSPA could be considered to be a bridge deck sonar device.

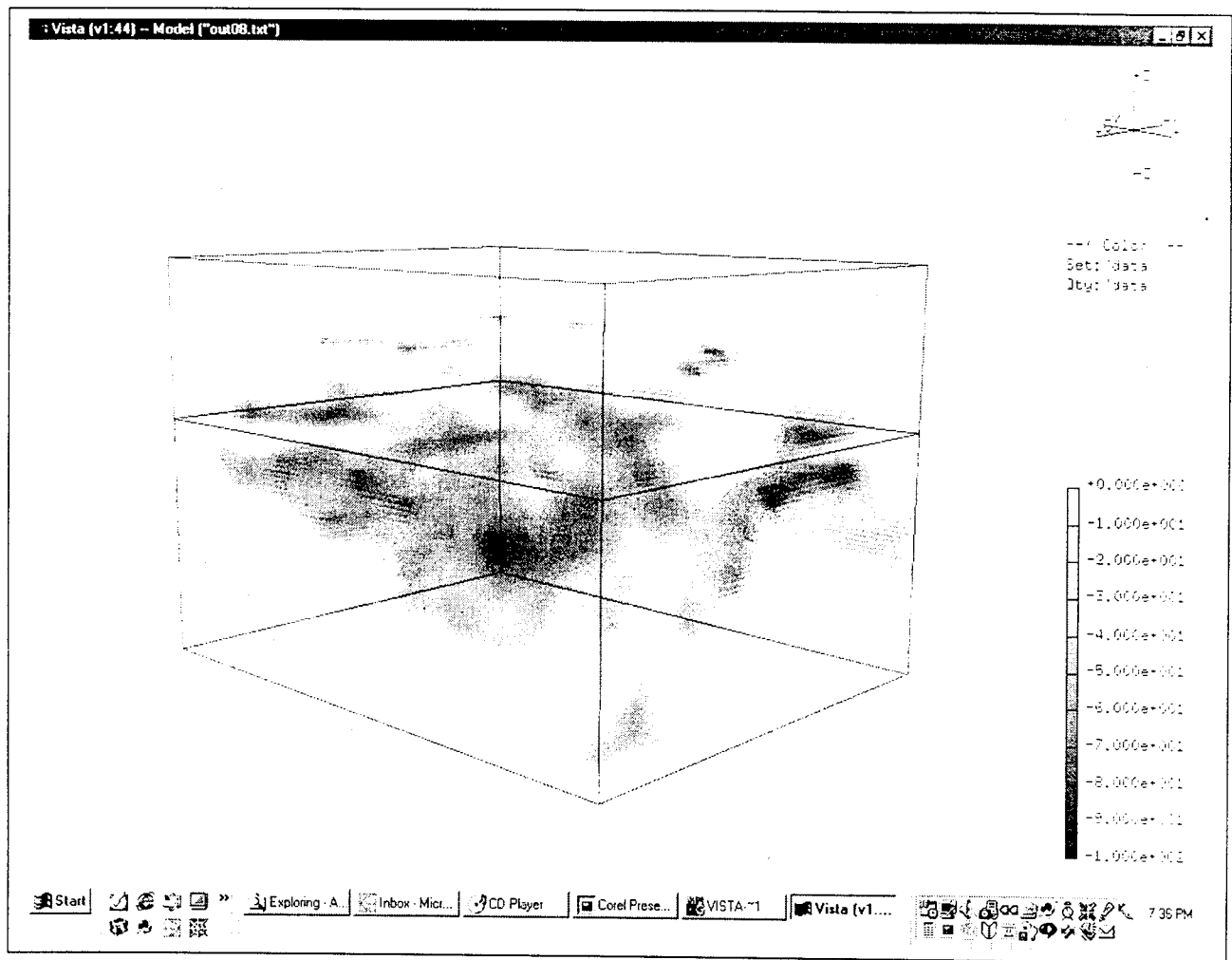


Figure 6.2. 3-dimensional thickness spectrum for a section of the Rt. I-287S bridge deck.

DELAMINATION
LEVEL - 8-12 cm

DECK BOTTOM
LEVEL - 15-19 cm

BELOW DECK ZONE -
APPARENT DEEP
REFLECTORS -
25-50 cm

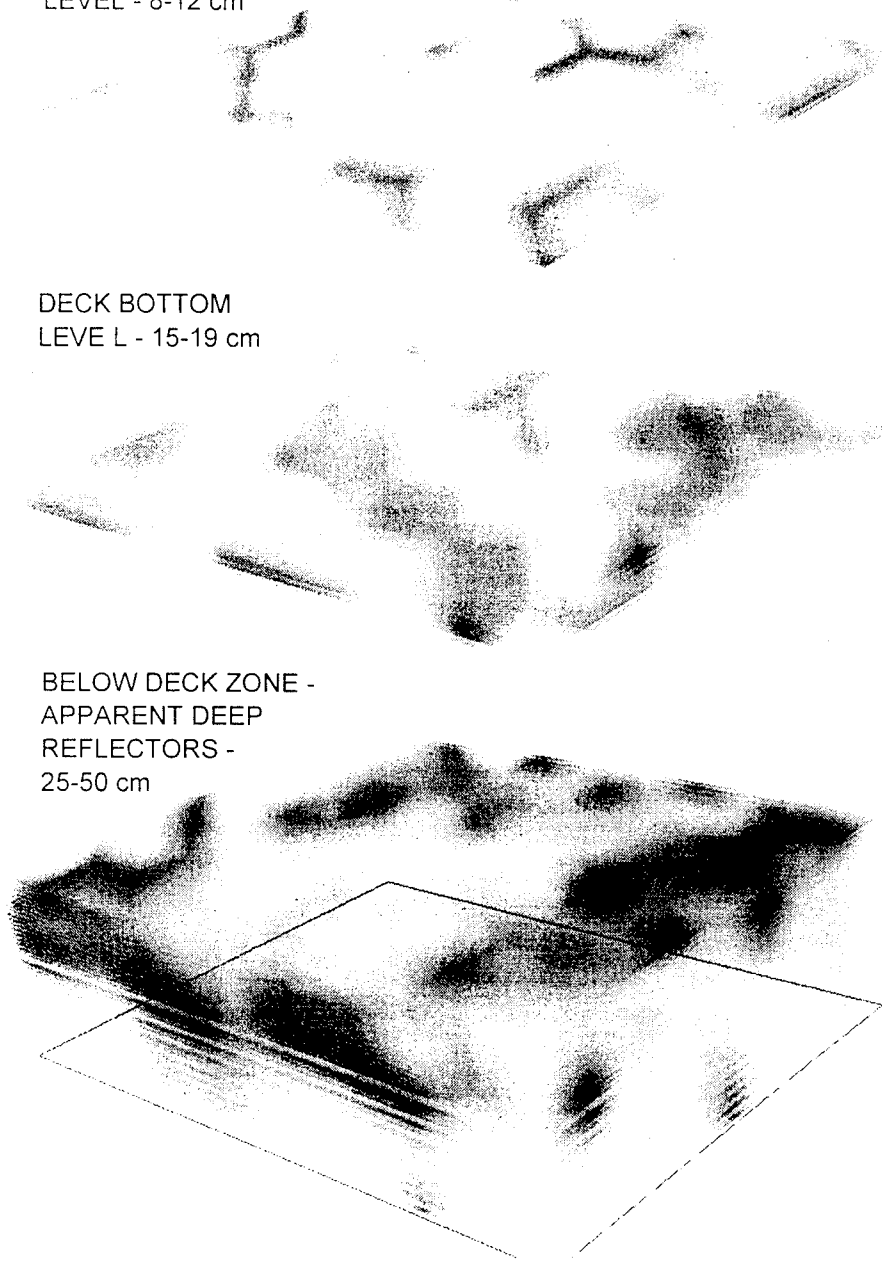


Figure 6.3. 3-dimensional thickness spectrum for a section of the Rt. I-287S bridge deck.

CHAPTER 7

CONCLUSIONS AND RECOMMENDATIONS

Ultrasonic seismic tests can be successfully used in long term post construction monitoring of changes in material quality and the deck condition with respect to deterioration caused by corrosion induced delamination. Material quality evaluation of bridge decks by integrated seismic devices is advantageous over the practice of core taking and testing because it is nondestructive and same locations can be periodically evaluated in an efficient, accurate and economical manner. Condition assessment with respect to the deck delamination by ultrasonic methods, the impact echo (IE) method in particular, is advantageous over the current practice of chain dragging. The primary reason for it is the ability of the IE method to detect zones of delamination at various stages, from initial to progressed and developed. This ability allows better prediction of deterioration processes in the deck, and thus presents a valuable tool for economic bridge management.

Ultrasonic testing of bridge decks can be successfully simulated by the finite element method. Some of the issues that require special attention include model discretization in the vicinity of the impact source (if axisymmetric models are used) and the description of damping. To improve quality of response spectra obtained from axisymmetric models, artificially strong surface wave components in the vicinity of the axis of symmetry (impact source) should be reduced by clipping of time histories (in the vertical direction). Results presented confirm the ability of the IE method to precisely determine the depth of the delamination, and to define the stage of a delamination induced deterioration. These effects are more pronounced at sensor locations closer to the impact source.

The finite element method was also successful in simulation of two probable scenarios of delamination progression: expansion\growth of a single small delamination, and progressive linking of several smaller delaminations. The two processes can be recognized through periodic monitoring of changes in amplitudes of peak frequencies for reflections from the delamination and the bottom of the deck, and for the flexural mode of oscillations. The growth of a delamination can be recognized by a growth of the delamination frequency peak, and a gradual shift of the full deck thickness peak towards a lower frequency flexible mode peak. The progressive crack linking process can be recognized by a growth of the delamination frequency peak, and a sudden transition from the full deck thickness peak to the frequency flexible mode peak as the delamination becomes continuous. The results point to a feasibility of the use of finite element simulations in the development of a neural network model for faster and more accurate condition assessment of bridge decks. This includes both improved evaluation of the degree of delamination, expressed through the size, position and continuity of the delamination, and better prediction of post construction deterioration processes.

Numerous improvements can be implemented that will improve both the accuracy and the speed of the bridge deck evaluation by the PSPA device. The duration of field testing, for example, can be significantly reduced through an implementation of a system consisting of a set of “lunch boxes” in a parallel connection. Both the accuracy and speed can be improved through incorporation of an automated data interpretation procedure based on numerical simulations and neural network models.

REFERENCES

- Gucunski, N. (1991), *Generation of Low Frequency Rayleigh Waves for Spectral Analysis of Surface Waves Method*, Ph.D. Dissertation, The University of Michigan, Ann Arbor.
- Gucunski, N. and A. Maher (1998), "Bridge Deck Condition Monitoring by Impact Echo Method," Proceedings of International Conference *MATEST '98 - Life Extension*, Brijuni, Croatia, October 1-2, 1998, 39-45.
- Hughes, T.J.R. (1987), *The Finite Element Method - Linear Static and Dynamic Finite Element Analysis*, Prentice-Hall, Englewood Cliffs, NJ.
- Nazarian, S., Stokoe, K.H., II, and W.R. Hudson (1983), "Use of Spectral Analysis of Surface Waves Method for Determination of Moduli and Thicknesses of Pavement Systems," *Transportation Research Record*, No. 930, National Research Council, Washington, D.C., 38-45.
- Nazarian, S. (1983), *In Situ Determination of Elastic Moduli of Soil Deposits and Pavement Systems by Spectral Analysis of Surface Waves Method*, Ph.D. Dissertation, University of Texas at Austin.
- Nazarian, S., Baker, M.R. & K. Crain (1993), *Development and Testing of a Seismic Pavement Analyzer*, Report SHRP-H-375, Strategic Highway Research Program, National Research Council, Washington, D.C.
- Nazarian, S. and D. Yuan (1997), "Evaluation and Improvement of Seismic Pavement Analyzer," Research Project 7-2936, The Center for Highway Materials Research, The University of Texas at El Paso, El Paso.

- Rojas, J., Nazarian, S., Tandon, V. & D. Yuan (1999), "Quality Management of Asphalt-Concrete Layers Using Wave Propagation Techniques," to appear in Proceedings of the AAPT Annual Meeting.
- Sansalone, M. J. (1993), "Detecting Delaminations in Concrete Bridge Decks with and without Asphalt Overlays Using an Automated Impact-Echo Field System," Proceedings of the British Institute of Non-Destructive Testing International Conference *NDT in Civil Engineering*, April 14-16, Liverpool, U.K., 807-820.
- Sansalone, M. J. and W. B. Street (1997), *Impact-Echo - Nondestructive Evaluation of Concrete and Masonry*, Bullbrier Press, Ithaca, New York.
- Stokoe II, H.K., Wright, S.G., Bay, J.A. & J.M. Roesset (1994), "Characterization of Geotechnical Sites by SASW Method," in R.D. Woods (ed) *Geotechnical Characterization of Sites*, Oxford and IBH Publ. Comp., New Delhi, India, 15-26.
- Zienkiewicz, O.C. and R.L. Taylor (1989), *The Finite Element Method*, 4th Edition, McGraw-Hill Book Comp., Maidenhead, England.

